Production and correlations of strange mesons and baryons at RHIC and LHC in hydrokinetic model

Yuri Sinyukov

Bogolyubov Institute, Kiev

In collaboration with
V.M. Shapoval

XII WPCF, Amsterdam, June 12-16 2017

Integrated HydroKinetic model: HKM → iHKM

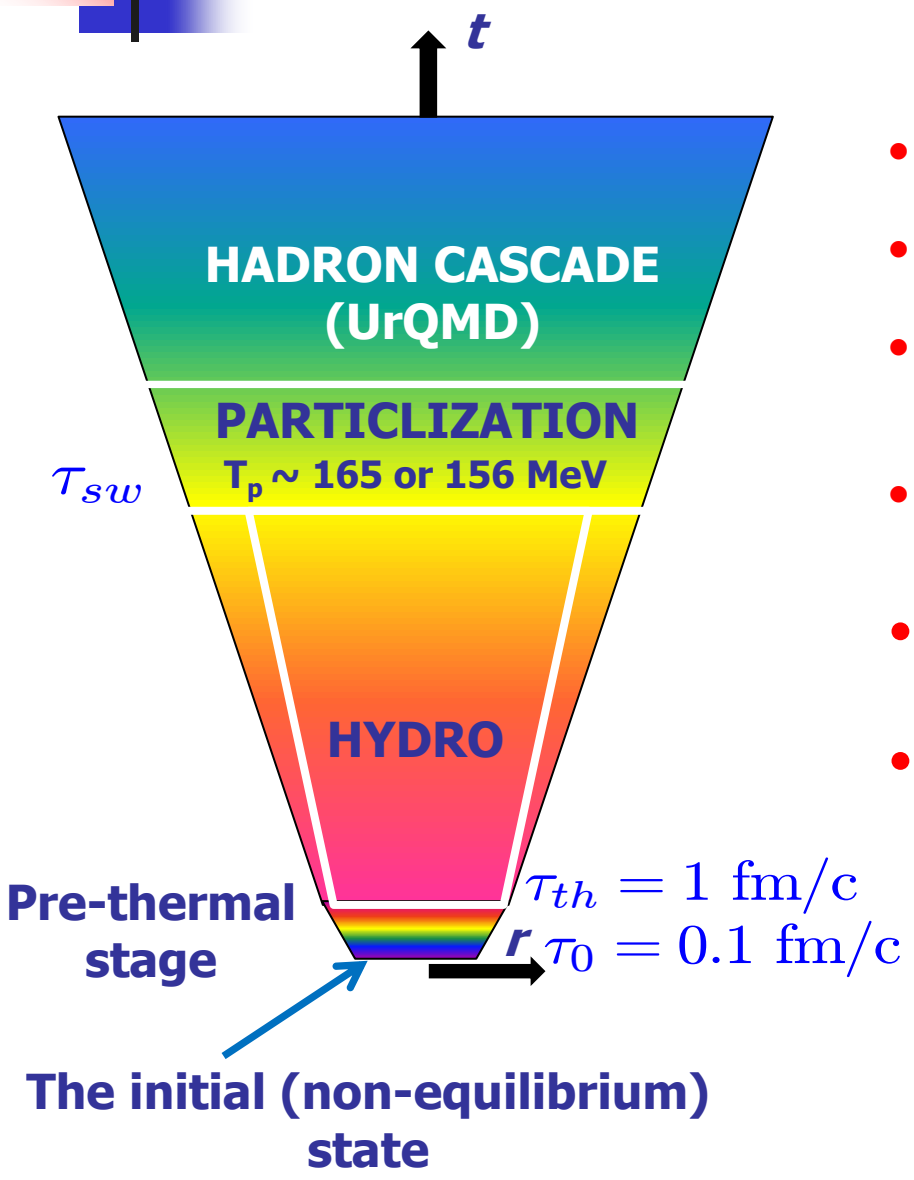

Complete algorithm incorporates the stages:

- **generation of the initial states;**
- **thermalization of initially non-thermal matter;**
- **viscous chemically equilibrated hydrodynamic expansion;**
- **sudden (with option: continuous) particlization of expanding medium;**
- **a switch to UrQMD cascade with near equilibrium hadron gas as input;**
- **simulation of observables.**

Yu.S., Akkelin, Hama: PRL 89 (2002) 052301;
… + Karpenko: PRC 78 (2008) 034906;
Karpenko, Yu.S. : PRC 81 (2010) 054903;
… PLB 688 (2010) 50;
Akkelin, Yu.S. : PRC 81 (2010) 064901;
Karpenko, Yu.S., Werner: PRC 87 (2013) 024914;
Naboka, Akkelin, Karpenko, Yu.S. : PRC **91** (2015) 014906;
Naboka, Karpenko, Yu.S. Phys. Rev. C **93** (2016) 024902.

.

MC-G Initial State (IS) attributed to $\tau_0 = 0.1$ fm/c

GLISSANDO 2

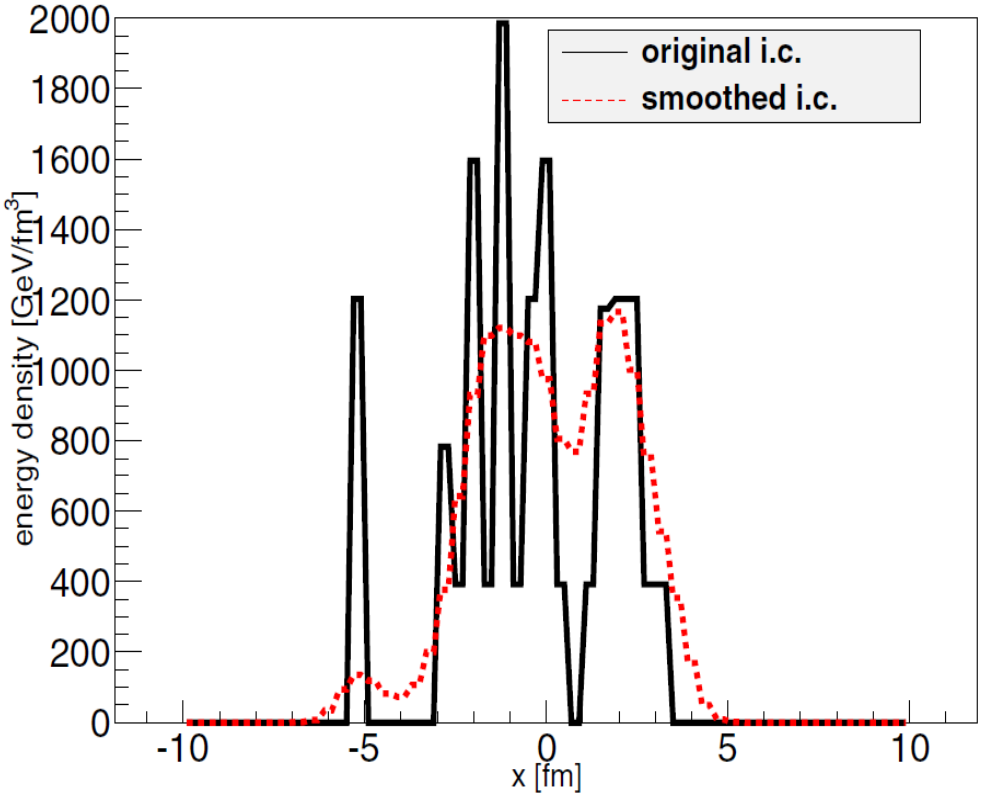

- The initial state (IS) is highly inhomogenious.
- It is not locally equilibrated.
- The IS most probable is strongly momentum anisotropic (result from CGC)

$$f(t_{\sigma_0}, \mathbf{r}_{\sigma_0}, \mathbf{p}) = \epsilon(b; \tau_0, \mathbf{r}_T) f_0(p)$$

$$T^{\mu\nu}_{\mathtt{free}}(x) = \int d^3p \frac{p^\mu p^\nu}{p_0} f_{\sigma_0}(x,p); \; T^{00}[f_0(p)] = 1$$

$$f_0^*(p) \propto \exp\left(-\sqrt{\frac{p_T^2}{\lambda_\perp^2} + \frac{p_L^2}{\lambda_\parallel^2}}\right)$$

Florkowski et al

MC-G Hybrid for ensemble of ISs :

$$\epsilon(b; \tau_0, \mathbf{r}_T) = \epsilon_0 \frac{(1-\alpha) N_W(b, \mathbf{r}_T)/2 + \alpha N_{bin}(b, \mathbf{r}_T)}{(1-\alpha) N_W(b=0, \mathbf{r}_T=0)/2 + \alpha N_{bin}(b=0, \mathbf{r}_T=0)}$$

Parameters of IS

$$\Lambda = \lambda_\perp / \lambda_\parallel$$

ϵ_0, α = 0.24

Multiplicity dependence of all charged particles on centrality

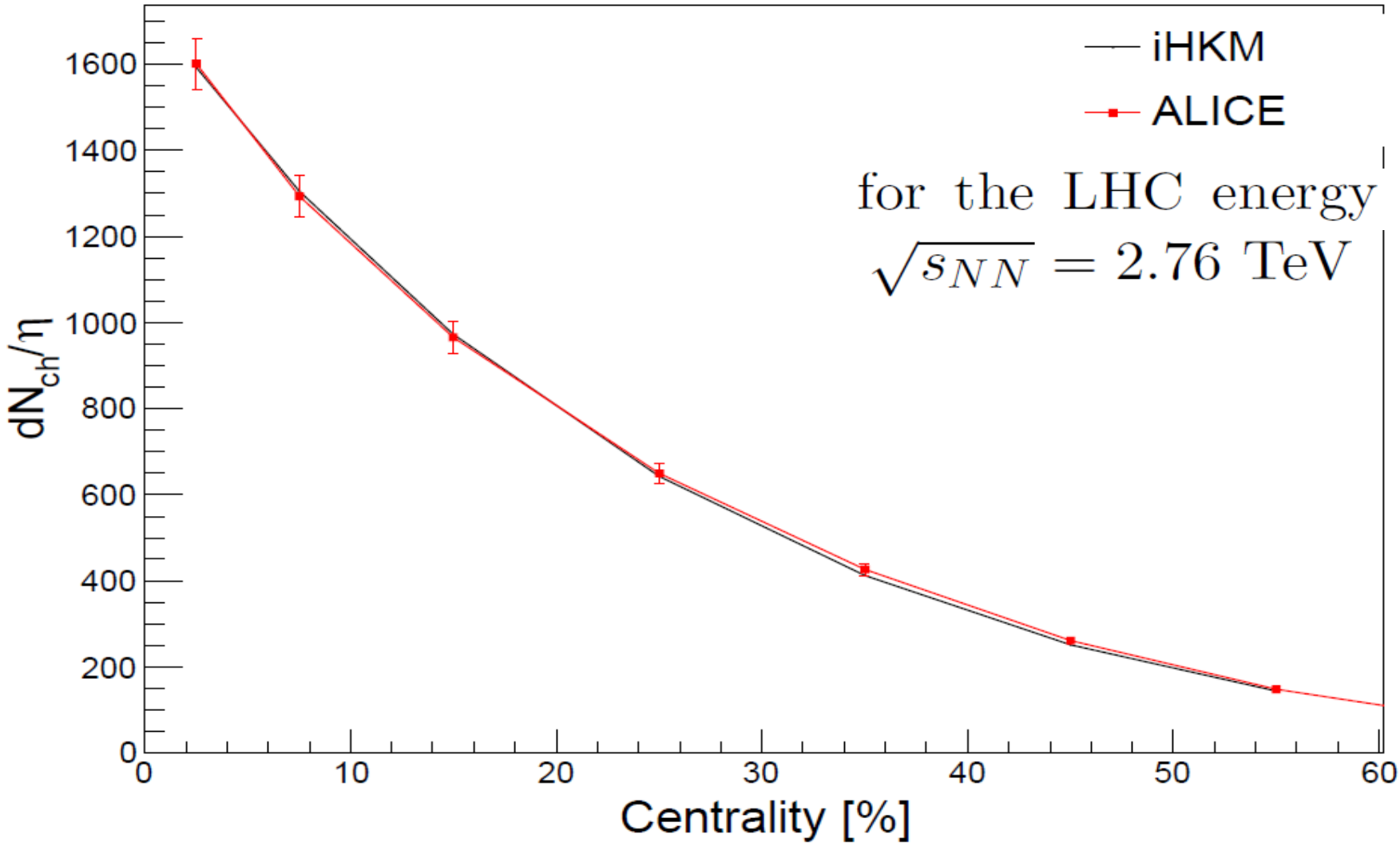

parameter values : $\tau_0 = 0.1$ fm/c, $\tau_{rel} = 0.25$ fm/c, $\eta/s = 0.08$, $\Lambda = 100$

Pre-thermal stage (thermalization)

Akkelin, Yu.S. :PRC **81** (2010); Naboka, Akkelin, Karpenko, Yu.S. : PRC **91** (2015).

Non-thermal state $\tau_0 = 0.1\ \mathrm{fm/c}$ $\longrightarrow$ locally near equilibrated state $\tau_{th} = 1\ \mathrm{fm/c}$

Boltzmann equation in relaxation time approximation (integral form)

MAIN OBJECT

$$\mathcal{P}_\sigma(x,p) = \exp\left(-\int_t^{t_\sigma} \frac{d\bar{t}}{\tau_{rel}(\overline{x},p)}\right)$$

$$\overline{x} \equiv (\bar{t}, \mathbf{x}_\sigma + (\mathbf{p}/p_0)(\bar{t} - t_\sigma))$$

Pre-thermal stage (thermalization)

Akkelin, Yu.S. :PRC **81** (2010); Naboka, Akkelin, Karpenko, Yu.S. : PRC **91** (2015).

Non-thermal state $\tau_0 = 0.1$ fm/c $\longrightarrow$ locally near equilibrated state $\tau_{th} = 1$ fm/c

Boltzmann equation in relaxation time approximation (integral form)

MAIN OBJECT

$$\mathcal{P}_\sigma(x,p) = \exp\left(-\int_t^{t_\sigma} \frac{d\bar{t}}{\tau_{rel}(\bar{x},p)}\right)$$

$$\bar{x} \equiv (\bar{t}, \mathbf{x}_\sigma + (\mathbf{p}/p_0)(\bar{t} - t_\sigma))$$

MAIN ANSATZ with minimal number of parameters: $\tau_0,\ \tau_{th},\ \tau_{rel}$

$$\mathcal{P}_{\tau_0\to\tau}(\tau) = \left(\frac{\tau_{th}-\tau}{t_{th}-\tau_0}\right)^{\frac{\tau_{th}-\tau_0}{\tau_{\rm rel}(\tau_0)}} \Longrightarrow T^{\mu\nu}(x) = T^{\mu\nu}_{\rm free}(x)\mathcal{P}(\tau) + T^{\mu\nu}_{\rm hyd}(x)(1-\mathcal{P}(\tau))$$

$$\Rightarrow 0 \le \mathcal{P}(\tau) \le 1,\ \mathcal{P}(\tau_0) = 1,\ \mathcal{P}(\tau_{th}) = 0,\ \partial_\mu \mathcal{P}(\tau)_{\tau_{\rm th}} = 0$$

Pre-thermal stage (thermalization)

Akkelin, Yu.S. :PRC **81** (2010); Naboka, Akkelin, Karpenko, Yu.S. : PRC **91** (2015).

Non-thermal state $\tau_0 = 0.1$ fm/c $\longrightarrow$ locally near equilibrated state $\tau_{th} = 1$ fm/c

Boltzmann equation in relaxation time approximation (integral form)

MAIN OBJECT

$$\mathcal{P}_\sigma(x,p) = \exp\Big(-\int_t^{t_\sigma} \frac{d\bar{t}}{\tau_{rel}(\bar{x},p)}\Big)$$

$$\bar{x} \equiv (\bar{t}, \mathbf{x}_\sigma + (\mathbf{p}/p_0)(\bar{t} - t_\sigma))$$

MAIN ANSATZ with minimal number of parameters: $\tau_0,\ \tau_{th},\ \tau_{rel}$

$$\mathcal{P}_{\tau_0\to\tau}(\tau) = \left(\frac{\tau_{th}-\tau}{t_{th}-\tau_0}\right)^{\frac{\tau_{th}-\tau_0}{\tau_{\rm rel}(\tau_0)}} \Longrightarrow T^{\mu\nu}(x) = T^{\mu\nu}_{\rm free}(x)\mathcal{P}(\tau) + T^{\mu\nu}_{\rm hyd}(x)(1-\mathcal{P}(\tau))$$

$$\Longrightarrow 0 \le \mathcal{P}(\tau) \le 1,\ \mathcal{P}(\tau_0) = 1,\ \mathcal{P}(\tau_{th}) = 0,\ \partial_\mu \mathcal{P}(\tau)_{\tau_{\rm th}} = 0$$

MAIN EQUATIONS

$$\partial_{;\mu}\widetilde{T}^{\mu\nu}_{\rm hyd}(x) = -T^{\mu\nu}_{\rm free}(x)\partial_{;\mu}\mathcal{P}(\tau)$$

where $\begin{cases} \tilde{T}^{\mu\nu}_{\rm hyd} = [1-\mathcal{P}(\tau)]T^{\mu\nu}_{\rm hyd} \\ \widetilde{\pi}^{\mu\nu} = \pi^{\mu\nu}(1-\mathcal{P}) \end{cases}$

$$(1-\mathcal{P}(\tau))\left\langle u^\gamma \partial_{;\gamma}\frac{\widetilde{\pi}^{\mu\nu}}{(1-\mathcal{P}(\tau))}\right\rangle = -\frac{\widetilde{\pi}^{\mu\nu} - (1-\mathcal{P}(\tau))\pi^{\mu\nu}_{\rm NS}}{\tau_\pi} - \frac{4}{3}\widetilde{\pi}^{\mu\nu}\partial_{;\gamma}u^\gamma$$

The other stages: Hydro evolution, particlization, hadronic cascade

- **Hydro evolution:** $\tau \leq \tau_{th}$ $T^{\mu\nu}(x) = T^{\mu\nu}_{\rm free}(x)\mathcal{P}(\tau) + T^{\mu\nu}_{\rm hyd}(x)(1-\mathcal{P}(\tau)) \to T^{\mu\nu}_{\rm hyd}(x)$ $\tau \geq \tau_{th}$

$$= (\epsilon_{\rm hyd}(x) + p_{\rm hyd}(x) + \Pi)u^{\mu}_{\rm hyd}(x)u^{\nu}_{\rm hyd}(x) - (p_{\rm hyd}(x) + \Pi)g^{\mu\nu} + \pi^{\mu\nu}.$$

IC is the result of pre-thermal evolutuon reached at τ_{th}

Solving of Israel-Stewart Relativistic Viscous Fluid Dynamics with Π=0

The other stages: Hydro evolution, particlization, hadronic cascade

- **Hydro evolution:** $\tau \leq \tau_{th}$ $\tau \geq \tau_{th}$

$$T^{\mu\nu}(x) = T^{\mu\nu}_{\rm free}(x)\mathcal{P}(\tau) + T^{\mu\nu}_{\rm hyd}(x)(1-\mathcal{P}(\tau)) \rightarrow T^{\mu\nu}_{\rm hyd}(x)$$
$$= (\epsilon_{\rm hyd}(x) + p_{\rm hyd}(x) + \Pi)u^{\mu}_{\rm hyd}(x)u^{\nu}_{\rm hyd}(x)$$
$$- (p_{\rm hyd}(x) + \Pi)g^{\mu\nu} + \pi^{\mu\nu}.$$

Solving of Israel-Stewart Relativistic Viscous Fluid Dynamics with $\prod$ =0

- **Particlization:**

at the isotherm hypersurface T=165 MeV

energy density $\epsilon = 0.5$ GeV/fm^3 for the Laine-Schroeder EoS

Switching hypersurface build with help of Cornelius routine.

For particle distribution the Grad's 14 momentum ansatz is used:

$$\frac{d^3\Delta N_i}{dp^* d(cos\theta) d\phi} = \frac{\Delta\sigma^*_\mu p^{*\mu}}{p^{*0}} p^{*2} f_{eq}\left(p^{*0}; T, \mu_i\right)\left[1 + (1 \mp f_{eq})\frac{p^*_\mu p^*_\nu \pi^{*\mu\nu}}{2T^2(\epsilon + p)}\right]$$

The other stages: Hydro evolution, particlization, hadronic cascade

- **Hydro evolution:** $\tau \leq \tau_{th}$ $T^{\mu\nu}(x) = T^{\mu\nu}_{\rm free}(x)\mathcal{P}(\tau) + T^{\mu\nu}_{\rm hyd}(x)(1-\mathcal{P}(\tau)) \rightarrow T^{\mu\nu}_{\rm hyd}(x)$ $\tau \geq \tau_{th}$

$$= (\epsilon_{\rm hyd}(x) + p_{\rm hyd}(x) + \Pi)u^{\mu}_{\rm hyd}(x)u^{\nu}_{\rm hyd}(x) - (p_{\rm hyd}(x) + \Pi)g^{\mu\nu} + \pi^{\mu\nu}.$$

Solving of Israel-Stewart Relativistic Viscous Fluid Dynamics with $\Pi = 0$

- **Particlization:** at the isotherm hypersurface T=165 MeV

$$\text{energy density } \epsilon = 0.5 \text{ GeV/fm}^3 \text{ for the Laine-Schroeder EoS}$$

Switching hypersurface build with help of Cornelius routine.

For particle distribution the Grad's 14 momentum ansatz is used:

$$\frac{d^3\Delta N_i}{dp^* d(cos\theta) d\phi} = \frac{\Delta\sigma^*_\mu p^{*\mu}}{p^{*0}} p^{*2} f_{eq}\left(p^{*0}; T, \mu_i\right)\left[1 + (1 \mp f_{eq})\frac{p^*_\mu p^*_\nu \pi^{*\mu\nu}}{2T^2(\epsilon + p)}\right]$$

- **Hadronic cascade:** The above distribution function with Poisson distributions for each sort of particle numbers is the input for UrQMD cascade.

The other stages: Hydro evolution, particlization, hadronic cascade

- **Hydro evolution:** $\tau \leq \tau_{th}$ $T^{\mu\nu}(x) = T^{\mu\nu}_{\rm free}(x)\mathcal{P}(\tau) + T^{\mu\nu}_{\rm hyd}(x)(1-\mathcal{P}(\tau)) = T^{\mu\nu}_{\rm hyd}(x)$

$$= (\epsilon_{\rm hyd}(x) + p_{\rm hyd}(x) + \Pi)u^{\mu}_{\rm hyd}(x)u^{\nu}_{\rm hyd}(x) - (p_{\rm hyd}(x) + \Pi)g^{\mu\nu} + \pi^{\mu\nu}.$$

Solving of Israel-Stewart Relativistic Viscous Fluid Dynamics with Π =0

- **Particlization:** at the isotherm hypersurface T=165 MeV

$$\text{energy density } \epsilon = 0.5 \text{ GeV/fm}^3 \text{ for the Laine-Schroeder EoS}$$

Switching hypersurface build with help of Cornelius routine.

For particle distribution the Grad's 14 momentum ansatz is used:

$$\frac{d^3\Delta N_i}{dp^* d(cos\theta) d\phi} = \frac{\Delta\sigma^*_\mu p^{*\mu}}{p^{*0}} p^{*2} f_{eq}\left(p^{*0}; T, \mu_i\right)\left[1 + (1 \mp f_{eq})\frac{p^*_\mu p^*_\nu \pi^{*\mu\nu}}{2T^2(\epsilon + p)}\right]$$

- **Hadronic cascade:** The above distribution function with Poisson distributions for each sort of particle numbers is the input for UrQMD

Details are in: Naboka, Karpenko, Yu.S. C **93** (2016) 024902

Initial flows at t_0=1-2 fm/c and Ro/Rs ratio (Yu.S. Act.Phys.Polon. B **37** (2006) 3343

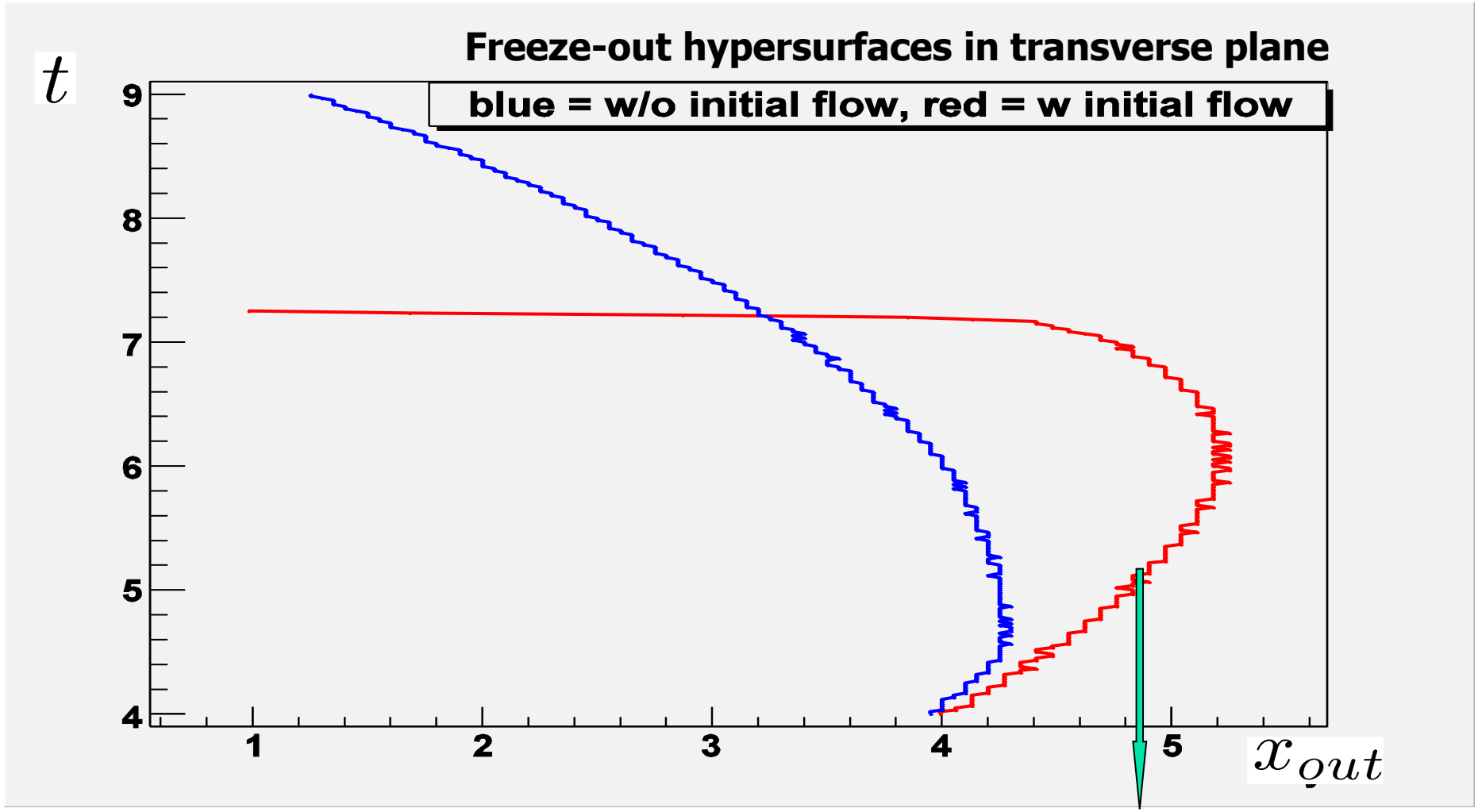

$$R^2_{out} \approx R^2_{side} + v^2\langle \triangle t^2 \rangle_p - 2v\langle \triangle x_{out} \triangle t \rangle_p, v = \frac{p_T}{p^0}$$

Emission functions for top SPS, RHIC and LHC energies

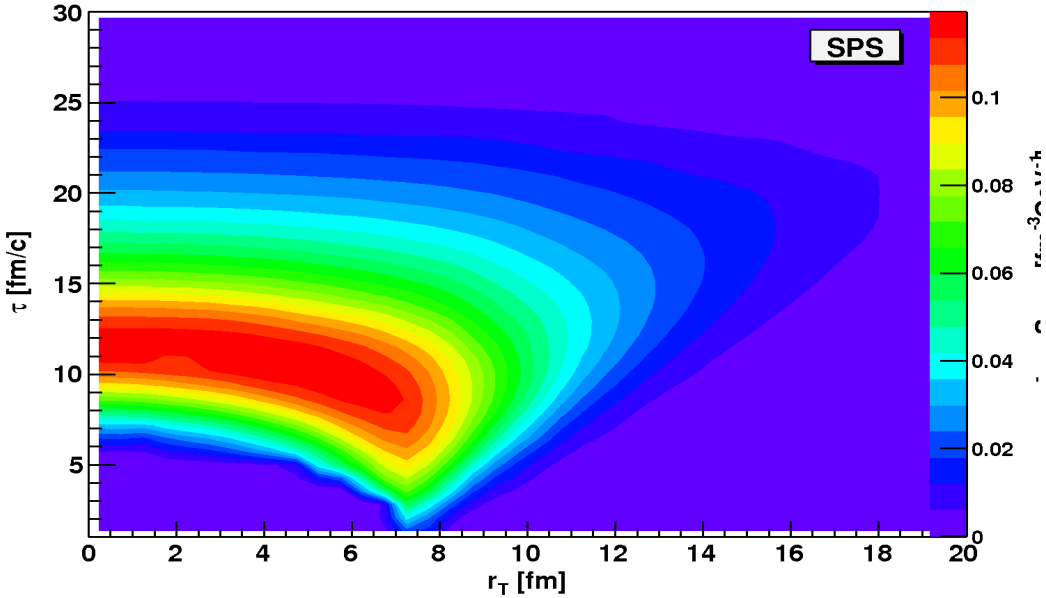

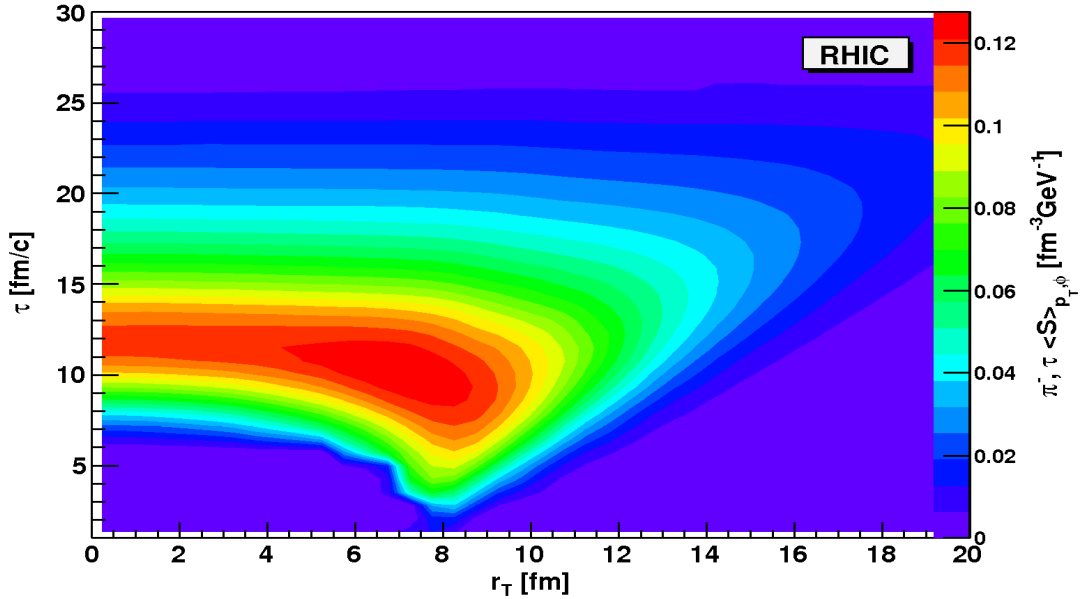

$$R^2_{out} \approx R^2_{side} + v^2\langle \triangle t^2 \rangle_p - 2v\langle \triangle x_{out} \triangle t \rangle_p, v = \frac{p_T}{p^0}$$

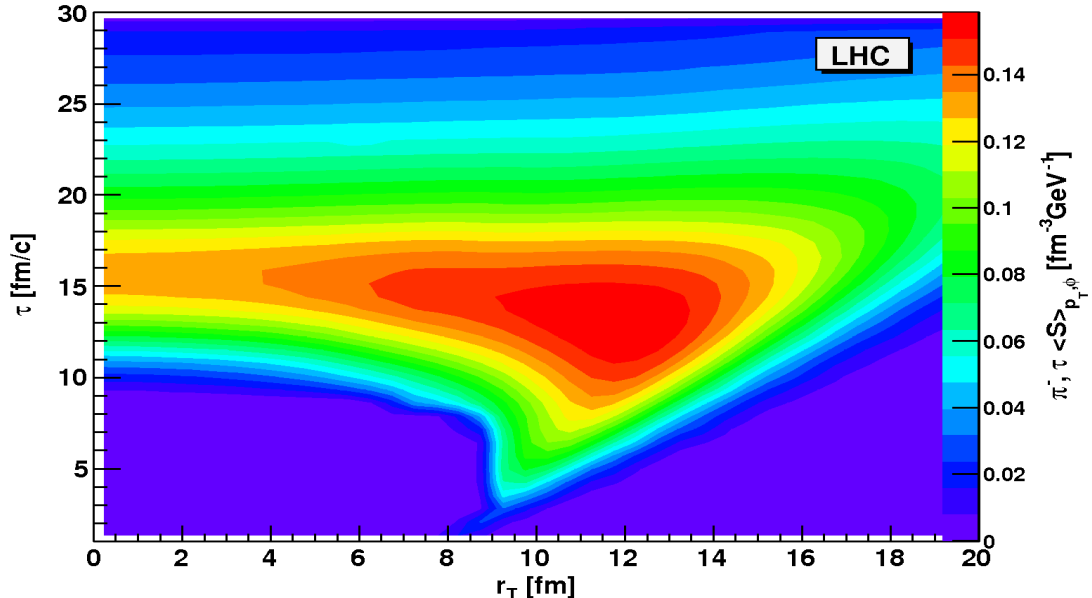

HKM prediction: solution of the HBT Puzzle

Two-pion Bose–Einstein correlations in central Pb–Pb collisions at $\sqrt{s_{NN}} = 2.76$ TeV ☆ ALICE Collaboration Physics Letters B 696 (2011) 328-

Quotations:

Available model predictions are compared to the experimental data in Figs. 2-d and 3. Calculations from three models incorporating a hydrodynamic approach, AZHYDRO [45], KRAKOW [46,47], and HKM [48,49], and from the hadronic-kinematics-based model HRM [50,51] are shown. An in-depth discussion is beyond the scope of this Letter but we notice that, while the increase of the radii between RHIC and the LHC is roughly reproduced by all four calculations, only two of them (KRAKOW and HKM) are able to describe the experimental R_{out}/R_{side} ratio.

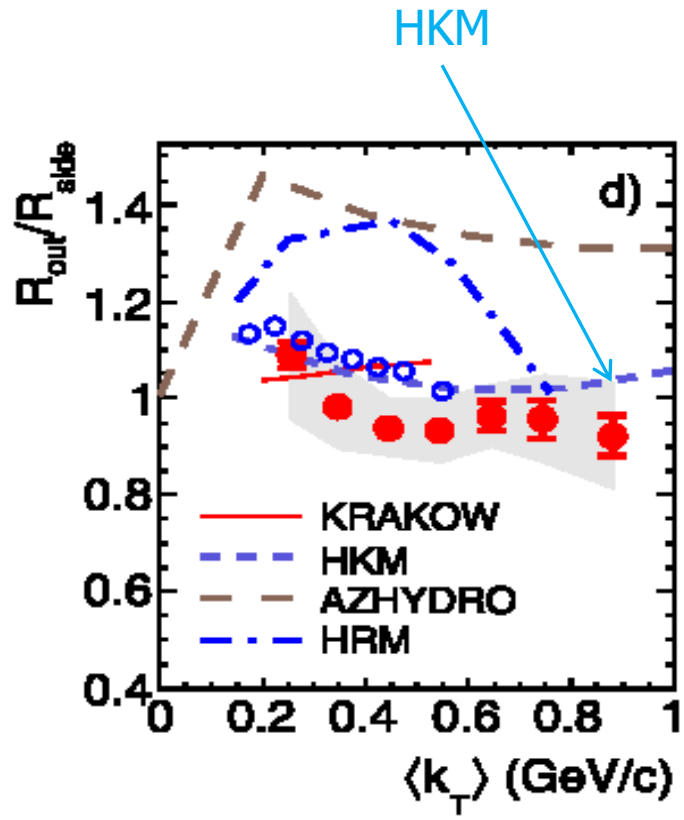

[48] I.A. Karpenko, Y.M. Sinyukov, Phys. Lett. B 688 (2010) 50.
[49] N. Armesto, et al. (Eds.), J. Phys. G 35 (2008) 054001.

Interferometry volume Vint in LHC p-p and **central** Au-Au, Pb-Pb collisions

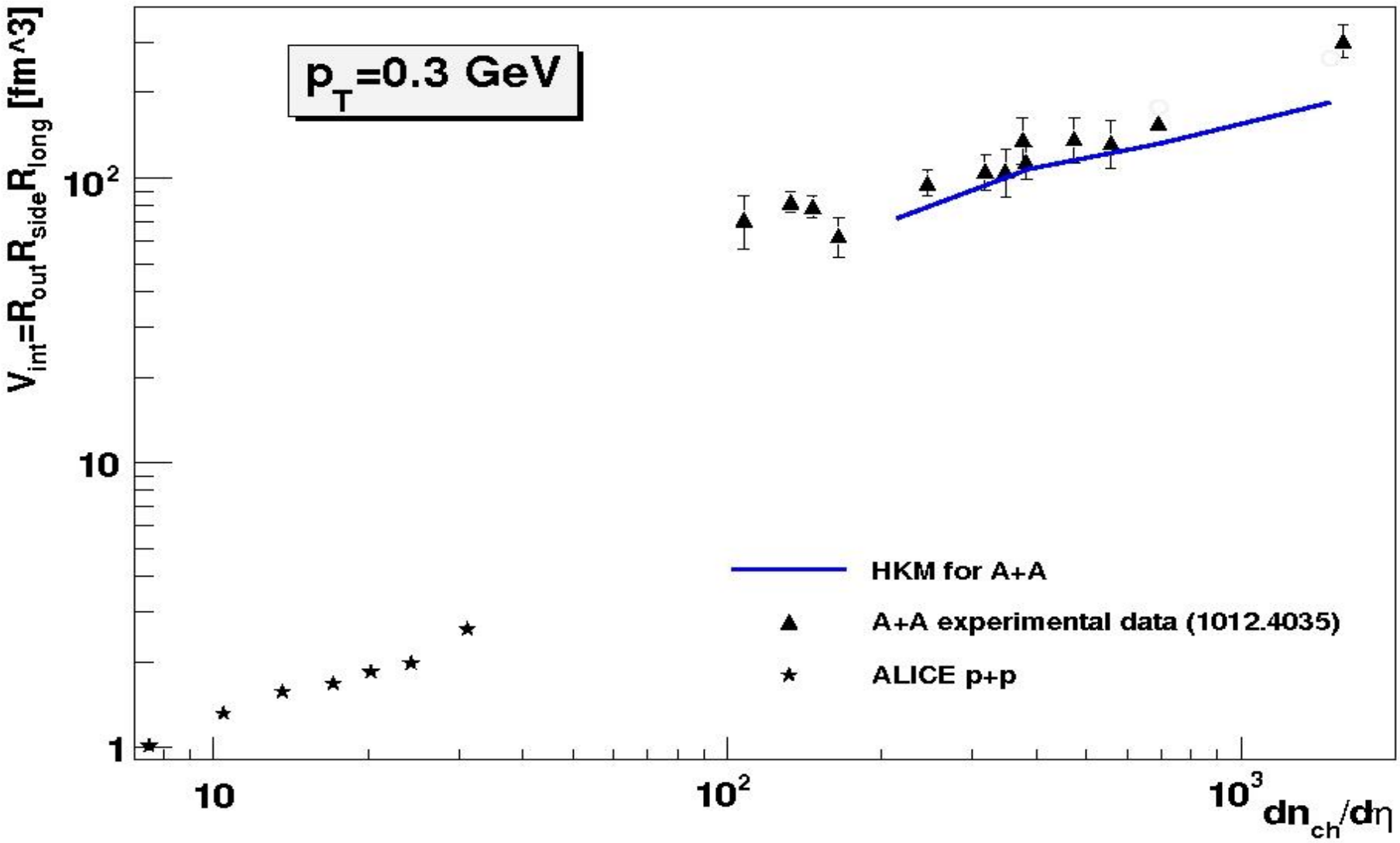

Interferometry volume Vint in LHC p-p and **central** Au-Au, Pb-Pb collisions

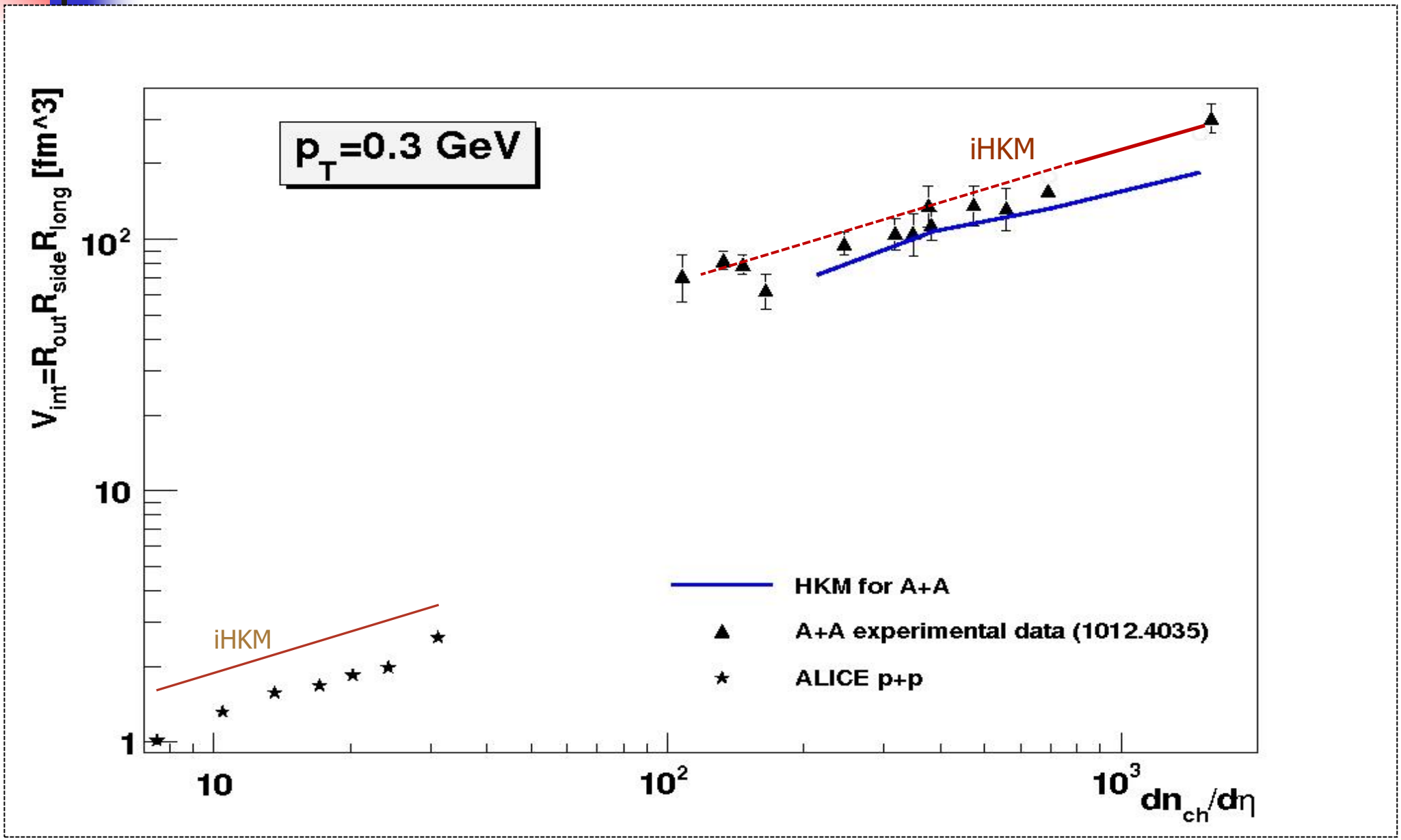

Interferometry volume Vint in LHC p-p and **central** Au-Au, Pb-Pb collisions

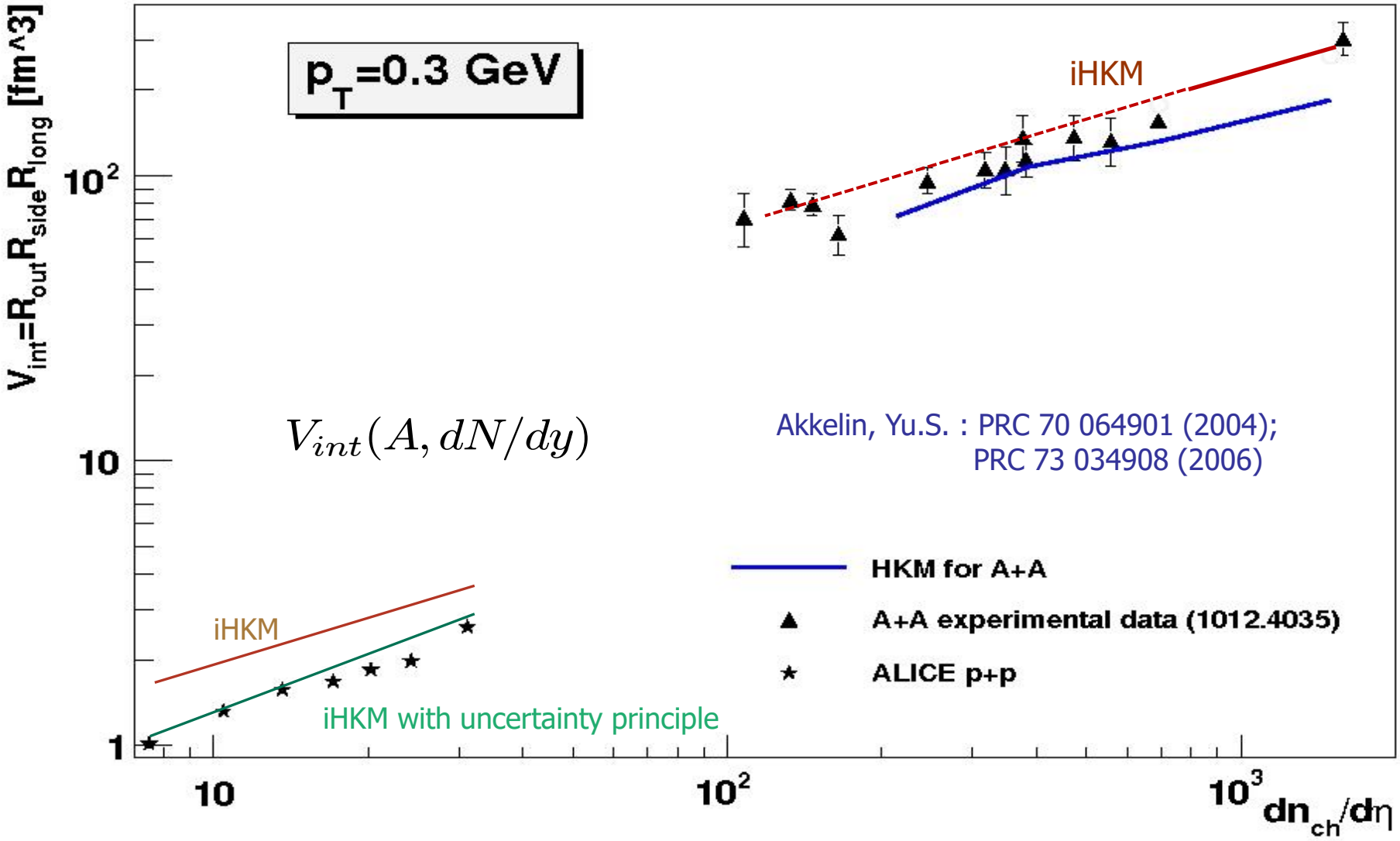

The iHKM parameters at Laine-Shroeder EoS

The $\frac{dN_{ch}}{d\eta}(c)$ is OK at fixed relative contribution of binary collision $\alpha = 0.24$.

but at different max initial energy densities when other parameters change:

The two values of the shear viscosity to entropy is used for comparison:

$$\eta/s = 0.08 \approx \frac{1}{4\pi} \text{ and } \eta/s = 0.2$$

The basic result (selected by red) is compared with results at other parameters, including viscous and ideal pure thermodynamic scenarios (starting at τ_0 without pre-thermal stage but with subsequent hadronic cascade).

Model	Λ	$\tau_{\rm rel}$	η/S	τ_0	$\langle \frac{\chi^2}{\rm ndf} \rangle$	ϵ_0 (GeV/fm^3)
Hydro			0	0.1	5.16	1076.5
Hydro			0.08	0.1	6.93	738.8
iHKM	1	0.25	0.08	0.1	3.35	799.5
iHKM	100	0.25	0.08	0.1	3.68	678.8
iHKM	100	0.75	0.08	0.1	3.52	616.5
iHKM	100	0.25	0.2	0.1	6.61	596.9
iHKM	100	0.25	0.08	0.5	5.36	126.7

The values τ_0, τ_{rel} corespond to fm/c.

No dramatic worsening of the results happens if simultaneously with changing of parameters/scenarios renormalize maximal initial energy density.

Equation of State - 1

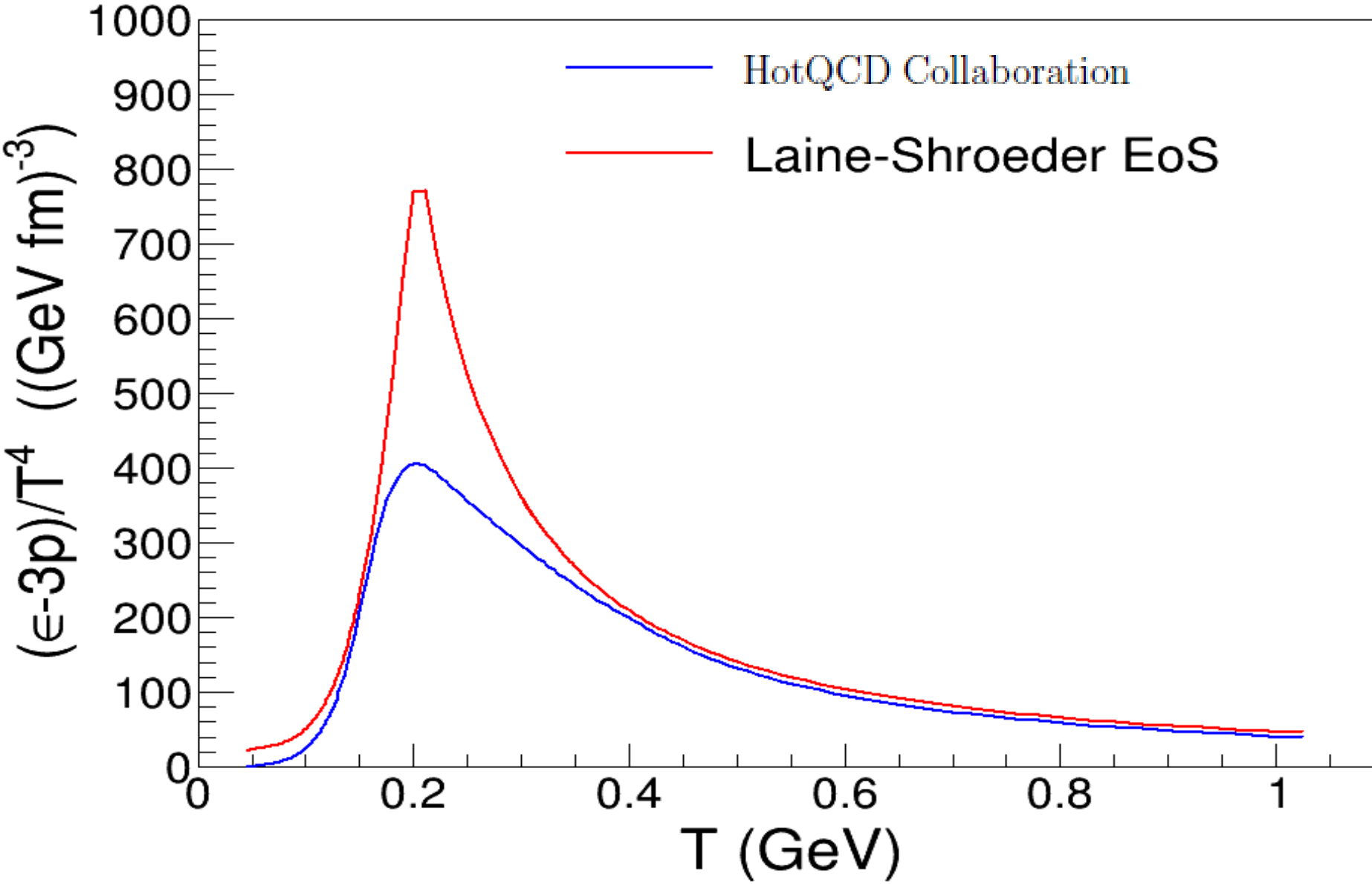

Equation of state -2

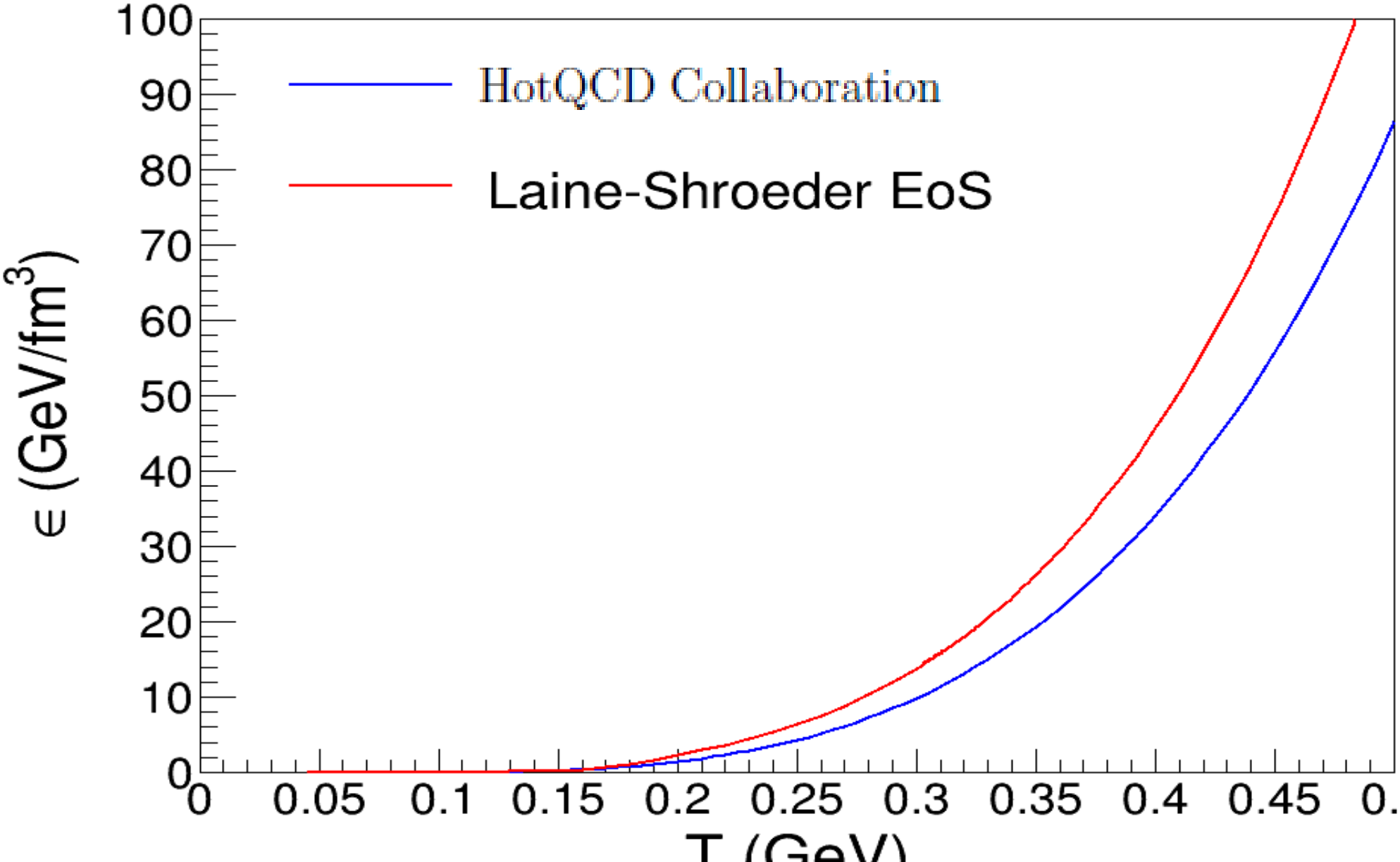

Continuous freeze-out **vs** sudden freeze-out

- Thermal models of particle production **vs** dynamic/evolutionary approaches

Kinetic/thermal freeze-out

Sudden freeze-out

Cooper-Frye prescription

$$p^0 \frac{d^3 N_i}{d^3 p} = \int_{\sigma_{th}} d\sigma_\mu p^\mu f_i(x,p)$$

The σ_{th} is typically isotherm.

Continuous freeze-out

$$p^0 \frac{d^3 N_i}{d^3 p} = \int d^4 x S_i(x,p) \approx \int_{\sigma(p)} d\sigma_\mu p^\mu f_i(x,p)$$

The $\sigma(p)$ is peace of hypersurface where the particles with momentum near p has a maximal emission rate.

Yu.S. *Phys. Rev.* **C78**,

Continuous freeze-out **vs** sudden freeze-out

- Thermal models of particle production **vs** dynamic/evolutionary approaches

Kinetic/thermal freeze-out

Sudden freeze-out

Cooper-Frye prescription

$$p^0 \frac{d^3 N_i}{d^3 p} = \int_{\sigma_{th}} d\sigma_\mu p^\mu f_i(x,p)$$

The σ_{th} is typically isotherm.

Continuous freeze-out

$$p^0 \frac{d^3 N_i}{d^3 p} = \int d^4 x S_i(x,p) \approx \int_{\sigma(p)} d\sigma_\mu p^\mu f_i(x,p)$$

The $\sigma(p)$ is peace of hypersurface where the particles with momentum near p has a maximal emission rate. ***Yu.S.*** *Phys. Rev.* **C78**,

Chemical freeze-out

$$N_i = \int_p \int_{\sigma_{ch}} \frac{d^3 p}{p^0} d\sigma_\mu p^\mu f_i\left(\frac{p^\mu u_\mu(x)}{T_{ch}}, \frac{\mu_{i,ch}}{T_{ch}}\right)$$

The numbers of quasi-stable particles is defined from N_i with taking into account the resonance decays but **not** inelastic re-scattering.

The T_{ch} is the minimal temperature when the expanding system is still (near) in local thermal and chemical equilibrium. Below the hadronic cascade takes place: $T_{ch} \to T_{part}$. The inelastic reactions, annihilation processes in hadron-resonance gas change the quasi-particle yields in comparison with sudden chem. freeze-out.

Thermal models **vs** evolutionary approach

Basic matter properties:
thermodynamic **EoS**

Thermal **models**

Chemical freeze-out at $T_{ch} \approx T_h$

Particle number ratios $\{\frac{N_i}{N_j}\}$

Thermal models **vs** evolutionary approach

Basic matter properties: thermodynamic **EoS**

Thermal models

Chemical freeze-out at $T_{ch} \approx T_h$

Particle number ratios $\{\frac{N_i}{N_j}\}$

Evolutionary models

$\frac{dN_{charge}}{d\eta}(c)$

$\frac{dN_\pi}{p_T dp_T}$

High dense matter formation time τ_0

Max. energy density $\epsilon(\tau_0) \equiv \epsilon_0$

At the particlization temperature $T_{part} \approx T_h$ hydrodynamic evolution transforms (suddenly or continuously) into interact. hadron gas evolution with inelastic reaction including annihilation. It may change particle number ratios. So, "chemical freeze-out" is continuois in evolutionary models.
How can we check it?

Multiplicity dependence of all charged particles on centrality and spectra for LHC energy $\sqrt{s_{NN}} = 2.76$ TeV

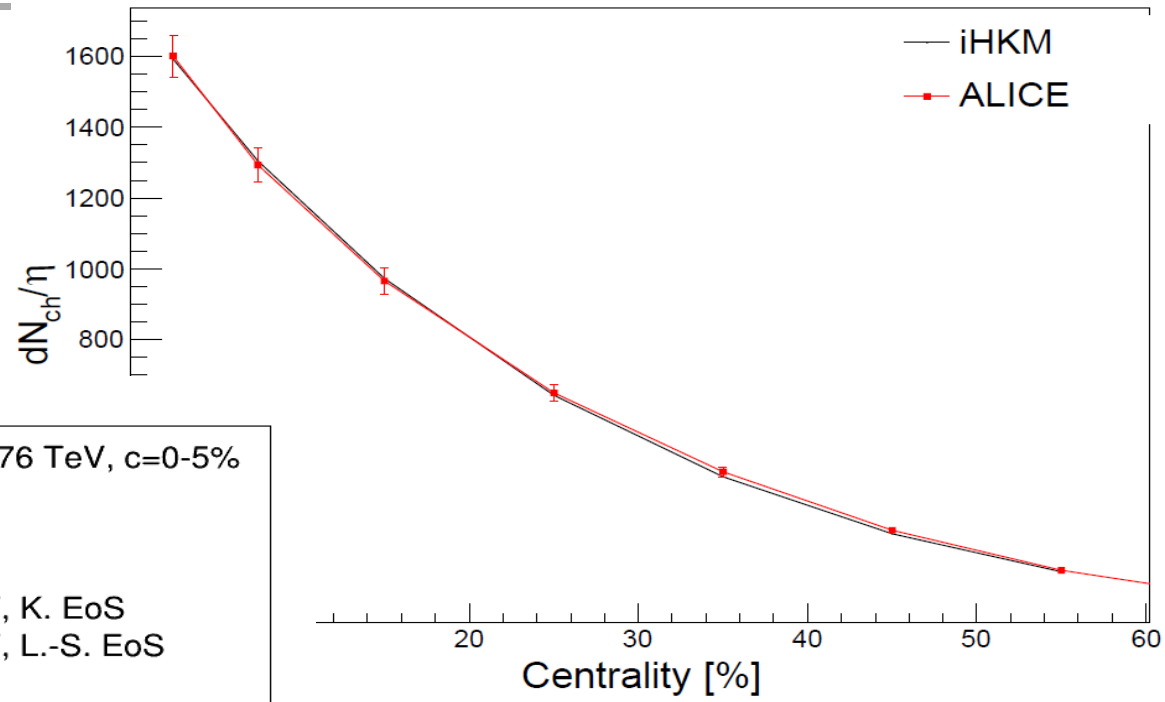

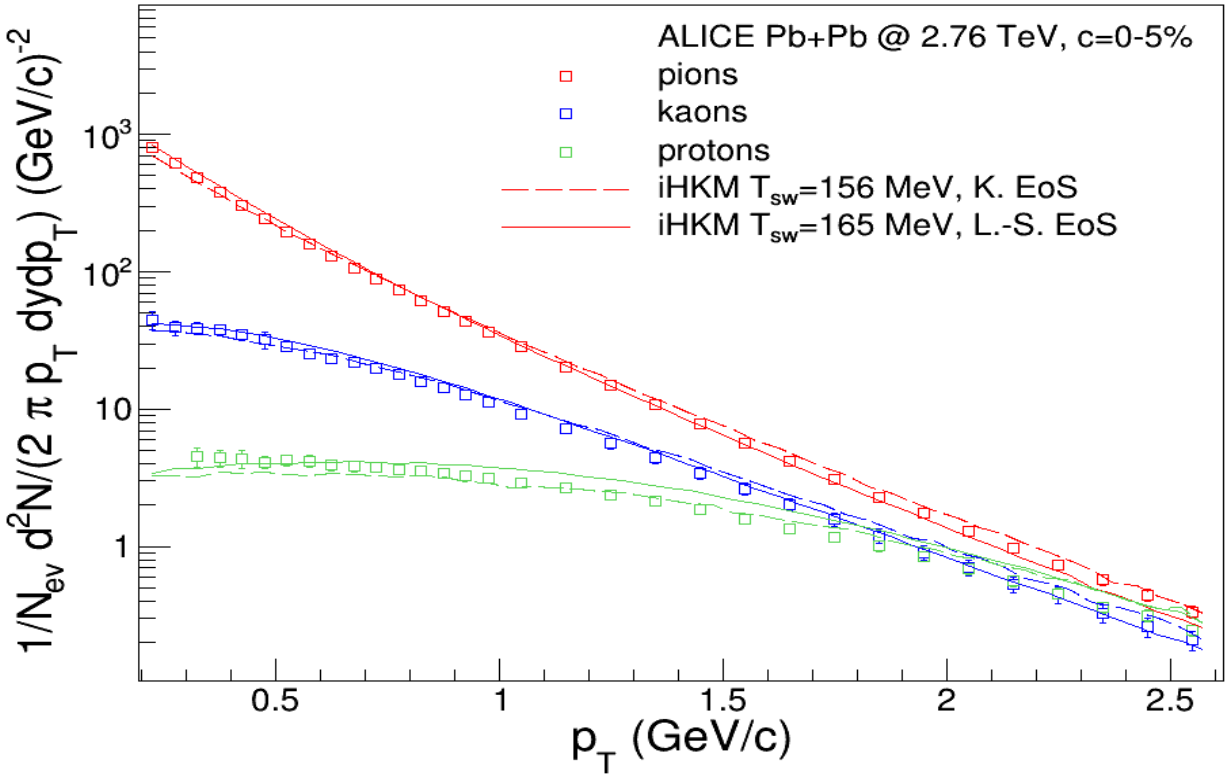

Thermal models **vs** evolutionary approach

Basic matter properties: thermodynamic **EoS**

Thermal models

Chemical freeze-out at $T_{ch} \approx T_h$

Particle number ratios $\{\frac{N_i}{N_j}\}$

Evolutionary models

$\frac{dN_{charge}}{d\eta}(c)$, $\frac{dN_\pi}{p_T dp_T}$

High dense matter formation time τ_0

Max. energy density $\epsilon(\tau_0) \equiv \epsilon_0$

At the particlization temperature $T_{part} \approx T_h$ hydrodynamic evolution transforms (suddenly or continuously) into interact. hadron gas evolution.

EoS: L.-S. → Karsch, Fodor (lattice QCD)

$T_h = 165 MeV \Rightarrow 156 MeV$

$\tau_0 = 0.1$ fm/c → 0.15 fm/c

$\epsilon_0 = 679$ GeV/fm^3 → 495 GeV/fm^3

iHKM

Thermal models **vs** evolutionary approach

Basic matter properties: thermodynamic **EoS**

Thermal models

Chemical freeze-out at $T_{ch} \approx T_h$

Particle number ratios $\{\frac{N_i}{N_j}\}$

Evolutionary models

$\frac{dN_{charge}}{d\eta}(c)$ $\frac{dN_\pi}{p_T dp_T}$

High dense matter formation time τ_0

Max. energy density $\epsilon(\tau_0) \equiv \epsilon_0$

At the particlization temperature $T_{part} \approx T_h$ hydrodynamic evolution transforms (suddenly or continuously) into interact. hadron gas evolution.

EoS: L.-S. ⟶ Karsch, Fodor (lattice QCD)

$T_h = 165 MeV \Longrightarrow 156 MeV$

$\tau_0 = 0.1$ fm/c ⟶ 0.15 fm/c

$\epsilon_0 = 679$ GeV/fm^3 ⟶ 495 GeV/fm^3

iHKM

Kinetic freeze-out

«Blast-wave" parametrization of sharp freeze-out hypersurface and transverse flows on it. Spectra $\frac{dN_i}{p_T dp_T} \longrightarrow T_{th}$

"Effective temperature" of maximal emission: $T_{th}(p)$

Anyway the kinetic freeze-out in evolutionary models is continuous, how can we check it?

Predictions for particle yield at LHC in central collisions from HKM

Pion, Kaon, and Proton Production in Central Pb–Pb Collisions at $\sqrt{s_{NN}} = 2.76$ TeV

The ALICE Collaboration **Phys. Rev. Lett. 109, 252301 (2012)**

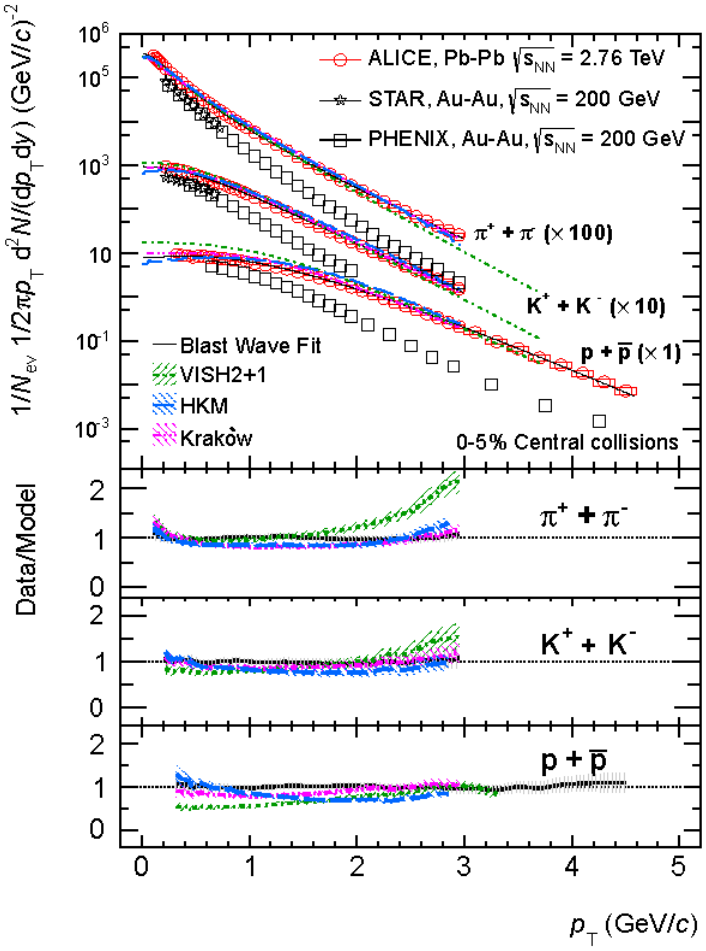

Quotations

This interpretation is supported by the comparison with HKM [39, 40], a similar model in which, after the hydrodynamic phase, particles are injected into a hadronic cascade model (UrQMD [41, 42]), which further transports them until final decoupling. The hadronic phase builds additional radial flow, mostly due to elastic interactions, and affects particle ratios due to inelastic interactions. HKM yields a better description of the data. At the LHC, hadronic final state interactions, and in particular antibaryon-baryon annihilation, may therefore be an important ingredient for the description of particle yields [43, 40], contradicting the scenario of negligible abundance-changing processes in the hadronic phase. The third model shown in Fig. 1 (Kraków [44, 45]) introduces non-equilibrium corrections due to viscosity at the transition from the hydrodynamic description to particles, which change the effective T_{ch}, leading to a good agreement with the data. In the region $p_T \lesssim 3$ GeV/c (Kraków) and $p_T \lesssim 1.5$ GeV/c (HKM) the last two models reproduce the experimental data within ~20%, supporting a hydrodynamic interpretation of the transverse momentum spectra at the LHC. These models also describe correctly other features of the space-time evolution of the system, as measured by ALICE with charged pion correlations [46].

[39] Y. Karpenko and Y. Sinyukov, J.Phys. **G38**, 124059 (2011), nucl-th/1107.3745.

[40] Y. Karpenko, Y. Sinyukov, and K. Werner, (2012), nucl-th/1204.5351.

Predictions for particle spectra at LHC in non-central collisions

Centrality Dependence of π, K, p in Pb–Pb at $\sqrt{s_{NN}} = 2.76$ TeV

ALICE Collaboration

arXiv:1303.0737v1 [hep-ex]

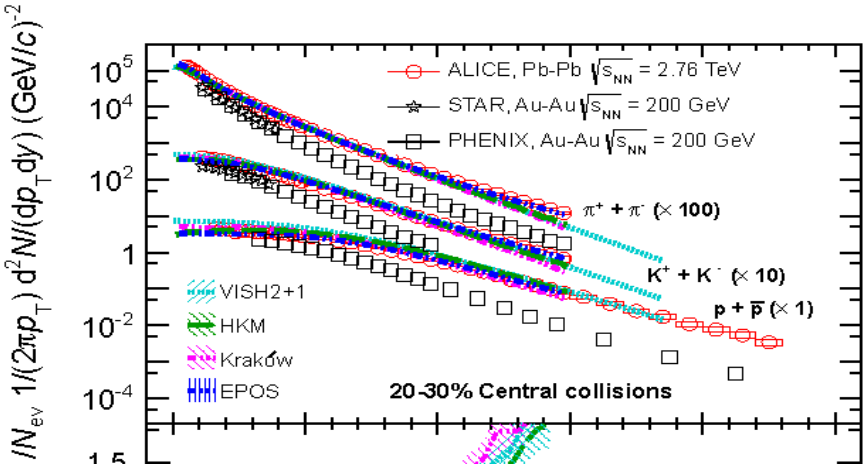

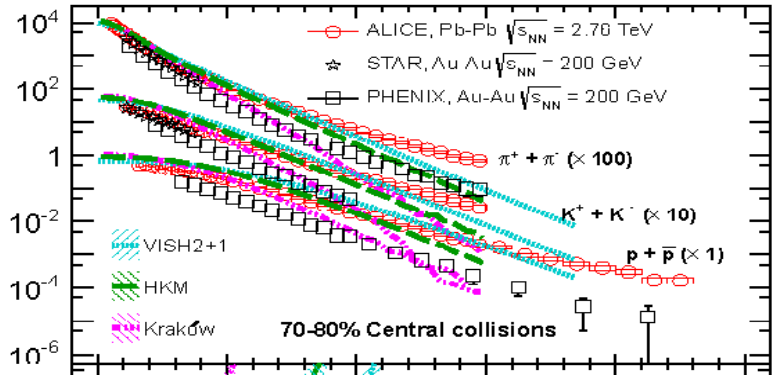

Quotations:

The difference between VISH2+1 and the data are possibly due to the lack of an explicit description of the hadronic phase in the model. This idea is supported by the comparison with HKM [47, 50]. HKM is a model similar to VISH2+1, in which after the hydrodynamic phase particles are injected into a hadronic cascade model (UrQMD), which further transports them until final decoupling. The hadronic phase builds up additional radial flow and affects particle ratios due to the hadronic interactions. As can be seen, this model yields a better description of the data. The protons at low p_T, and hence their total number, are rather well reproduced, even if the slope is significantly smaller than in the data. Antibaryon-baryon annihilation is an important ingredient for the description of particle yields in this model [47, 50].

.....

Phys. Rev. C 87, 024914 (2013)

[47] Y. Karpenko, Y. Sinyukov, and K. Werner, (2012), arXiv:1204.5351 [nucl-th]

[50] Y. Karpenko and Y. Sinyukov, J.Phys.G **G38**, 124059 (2011).

Particle number ratios at the LHC

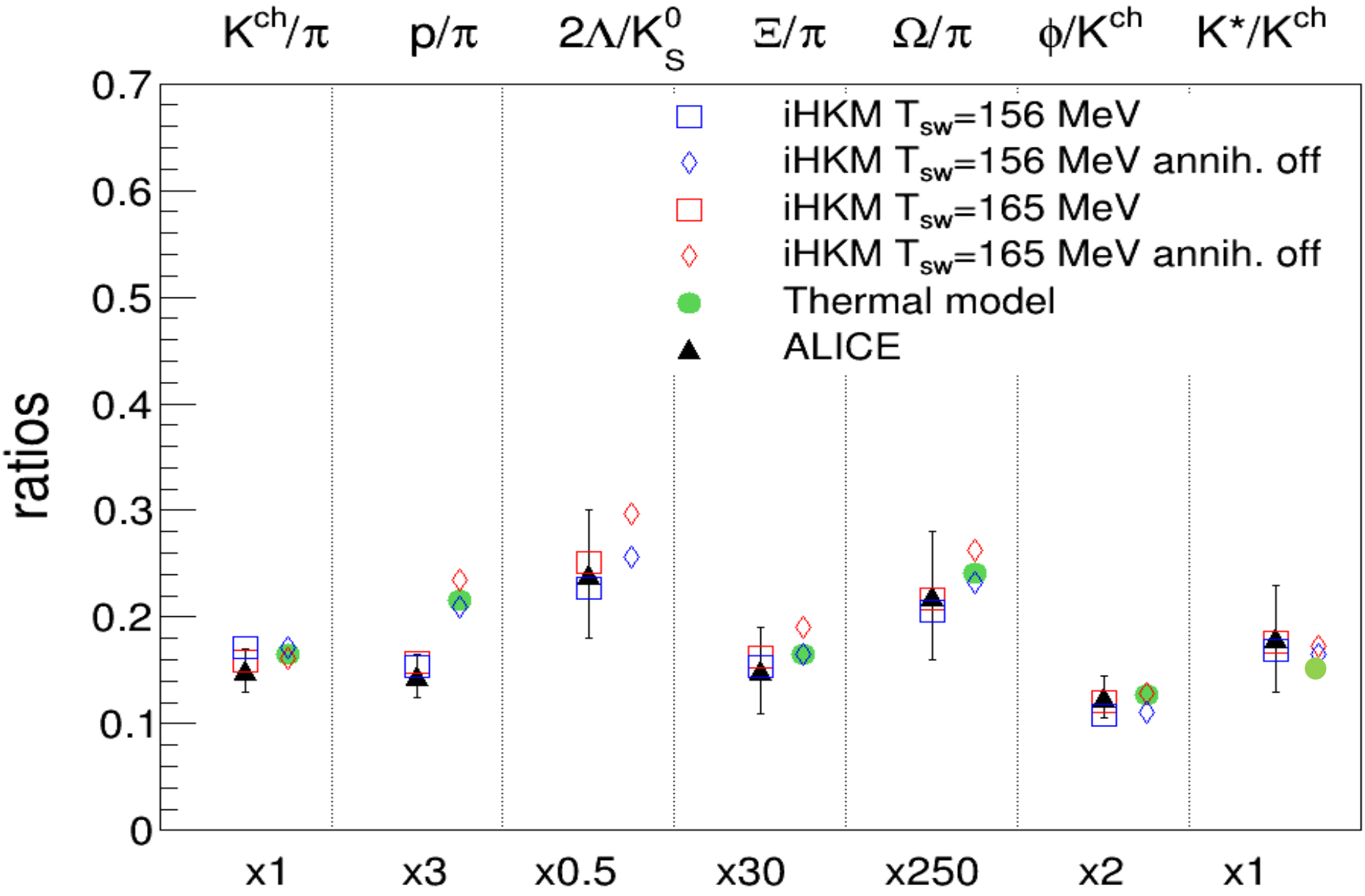

$K^{*0} \to K^{+}\pi^{-}$ radiation picture in iHKM.
Sudden vs continuous thermal freeze-out at the LHC.

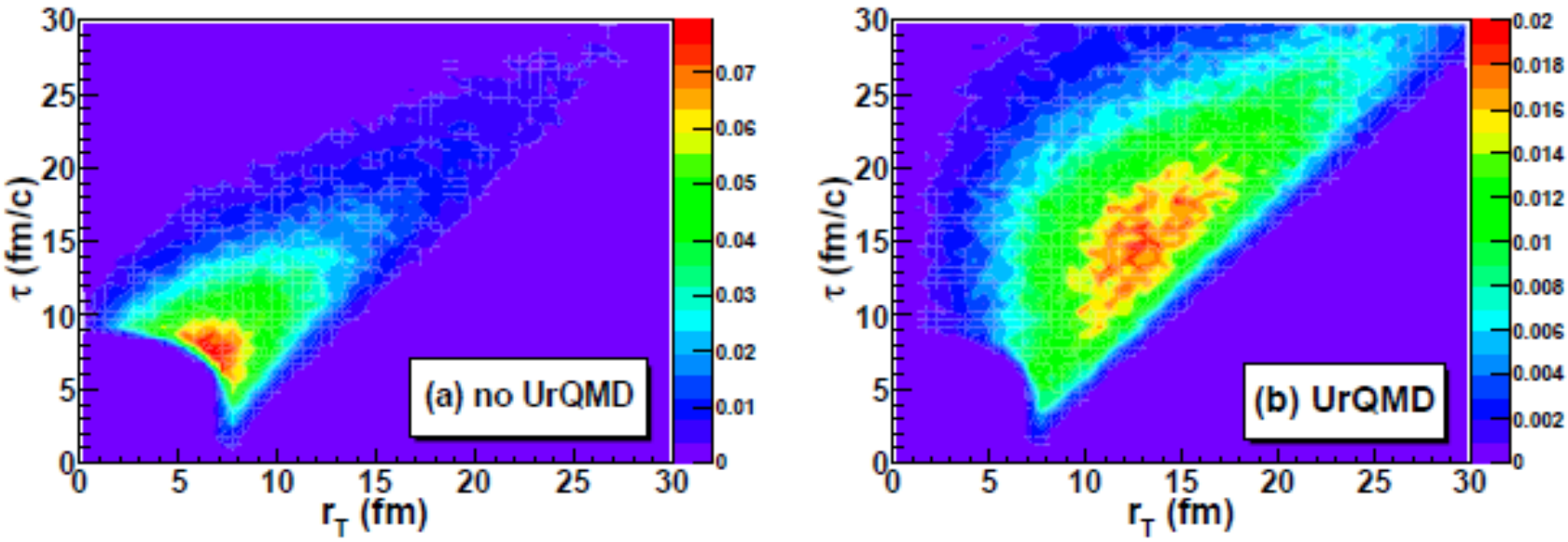

The comparison of the emission functions $g(\tau, r_T)$, averaged over complementary space and momentum components, of $K^{+}\pi^{-}$ pairs, associated with $K(892)^{*0}$ decay products, for two cases: (a) free-streaming of the particles and resonances, and (b) UrQMD hadron cascade. The plots are obtained using iHKM simulations of Pb+Pb collisions at the LHC $\sqrt{s_{NN}} = 2.76$ GeV, $0.3 < k_T < 5$ GeV/c, $|y| < 0.5$, $c = 5 - 10\%$.

Suppression of K^{*0} due to continuous thermal freeze-out (LHC)

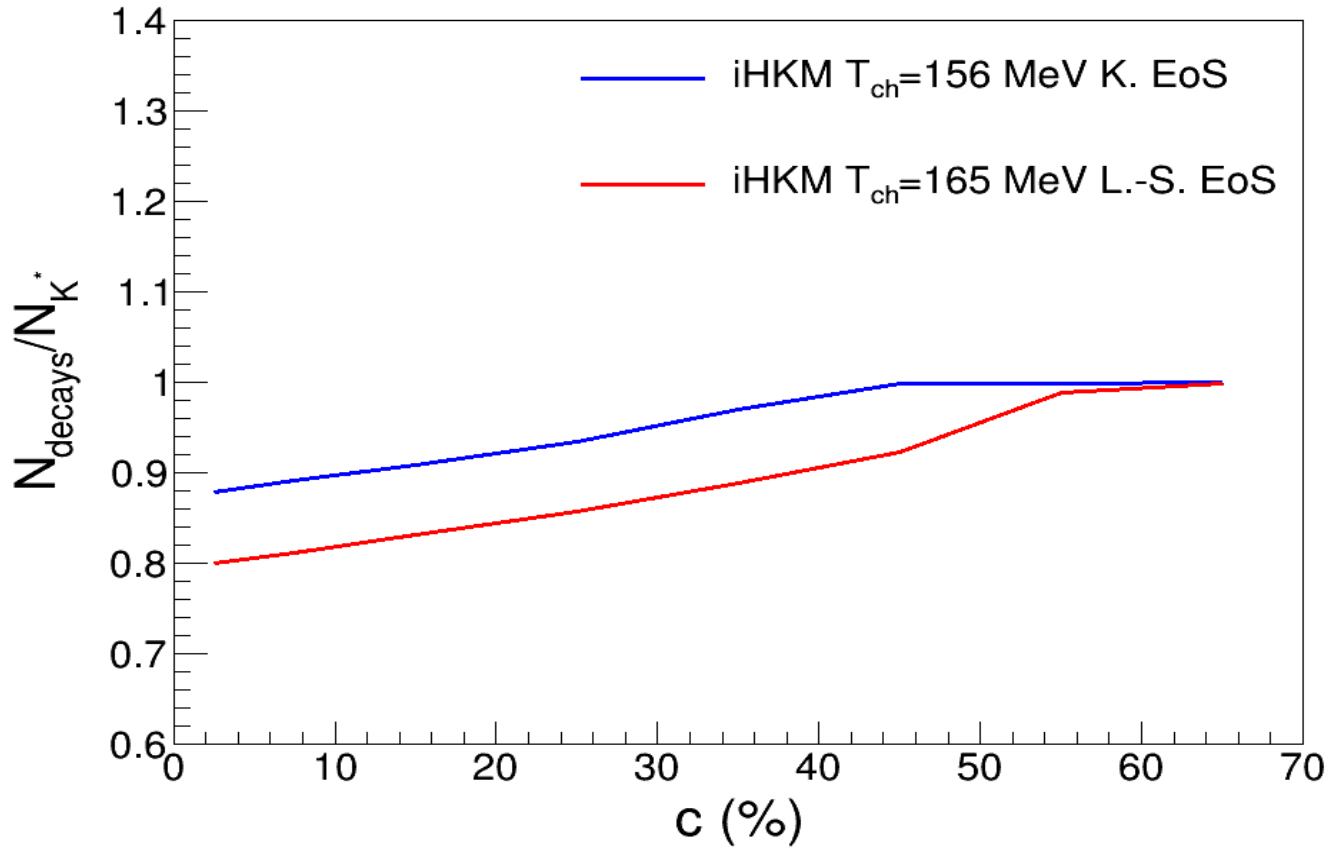

The fraction of $K^+\pi^-$ pairs coming from $K(892)^*$ decay, which can be identified as daughters of K^* in iHKM simulations after the particle rescattering stage modeled within UrQMD hadron cascade. The simulations correspond to LHC Pb+Pb collisions at $\sqrt{s_{NN}} = 2.76$ TeV with different centralities. The iHKM results are presented for two cases: the Laine-Shroeder equation of state with particlization temperature $T_p = 163$ MeV (red line) and the Karsch equation of state with $T_p = 156$ MeV (blue line).

Ratios to K (LHC)

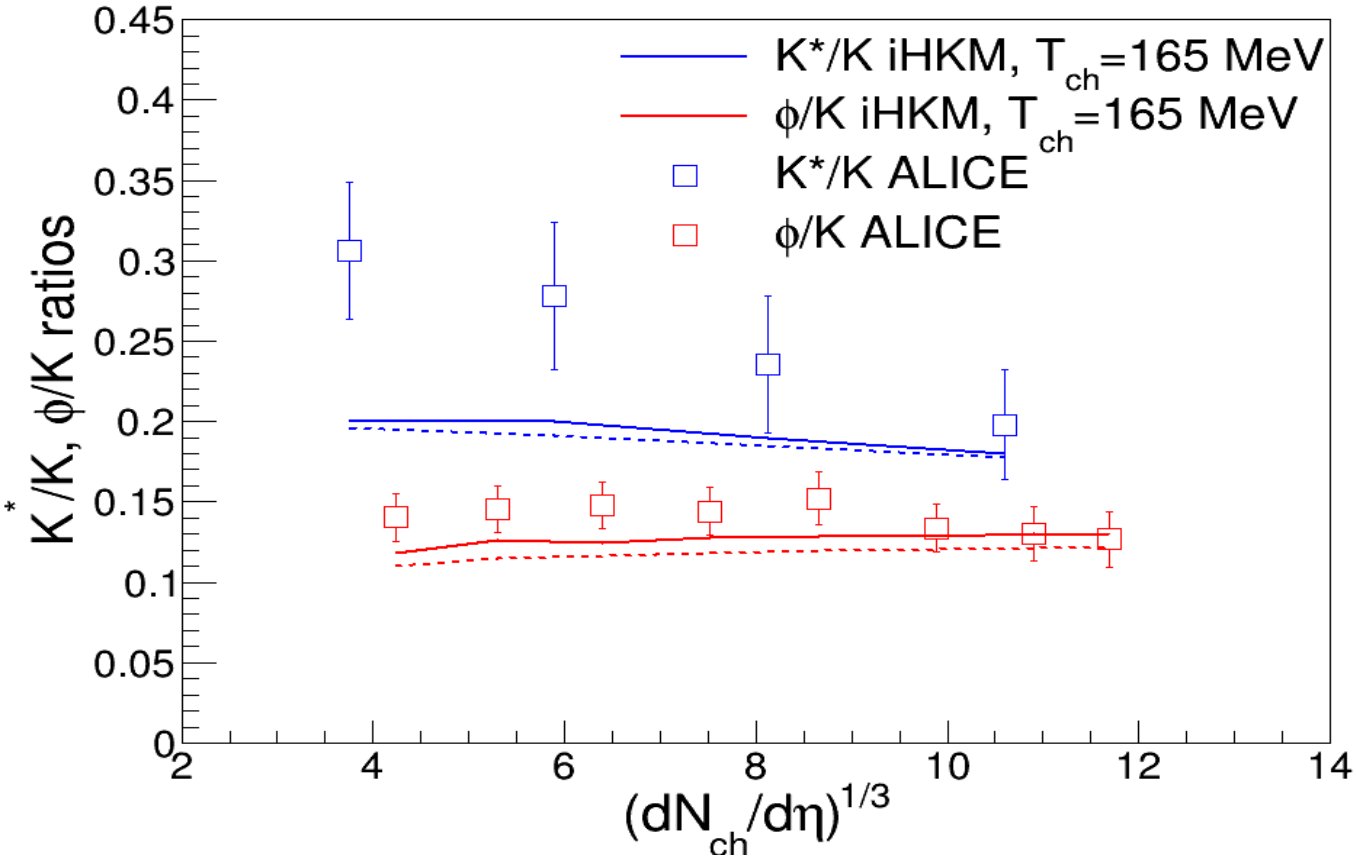

The comparison of K^*/K^+ and ϕ/K^+ ratios dependency on particle multiplicity $(dN_{ch}/d\eta)^{1/3}$ calculated in iHKM for the case of LHC Pb+Pb collisions at $\sqrt{s_{NN}} = 2.76$ TeV and the corresponding ALICE experimental data [6]. The solid lines correspond to the iHKM calculations, performed using hadronization temperature $T_{sw} = 163$ MeV and Laine-Shroeder equation of state [15], while the dashed lines are related to the Karsch equation of state [16] and $T_{sw} = 156$ MeV.

Ratios to K (RHIC)

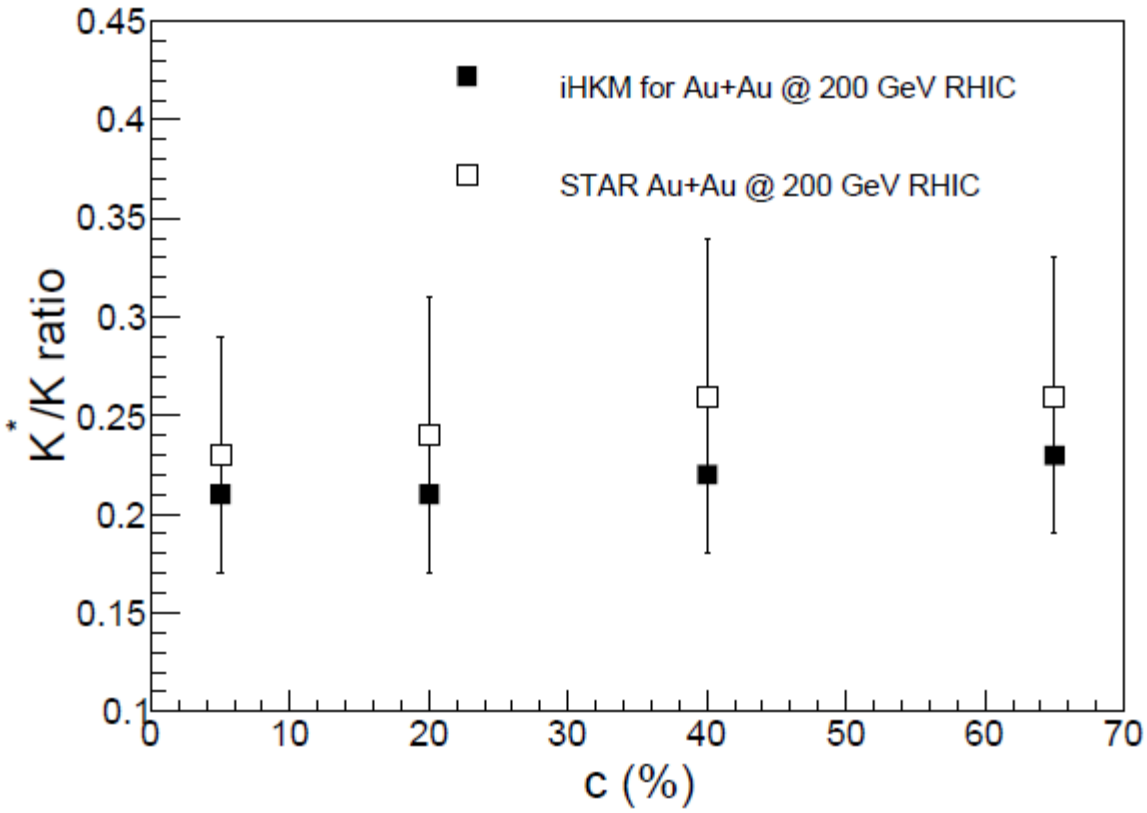

The comparison of K^*/K^+ ratio calculated in iHKM for the case of RHIC Au+Au collisions at $\sqrt{s_{NN}} = 200$ GeV and the experimental data [7] for different centrality classes.

Spectra of K^{*0} (LHC)

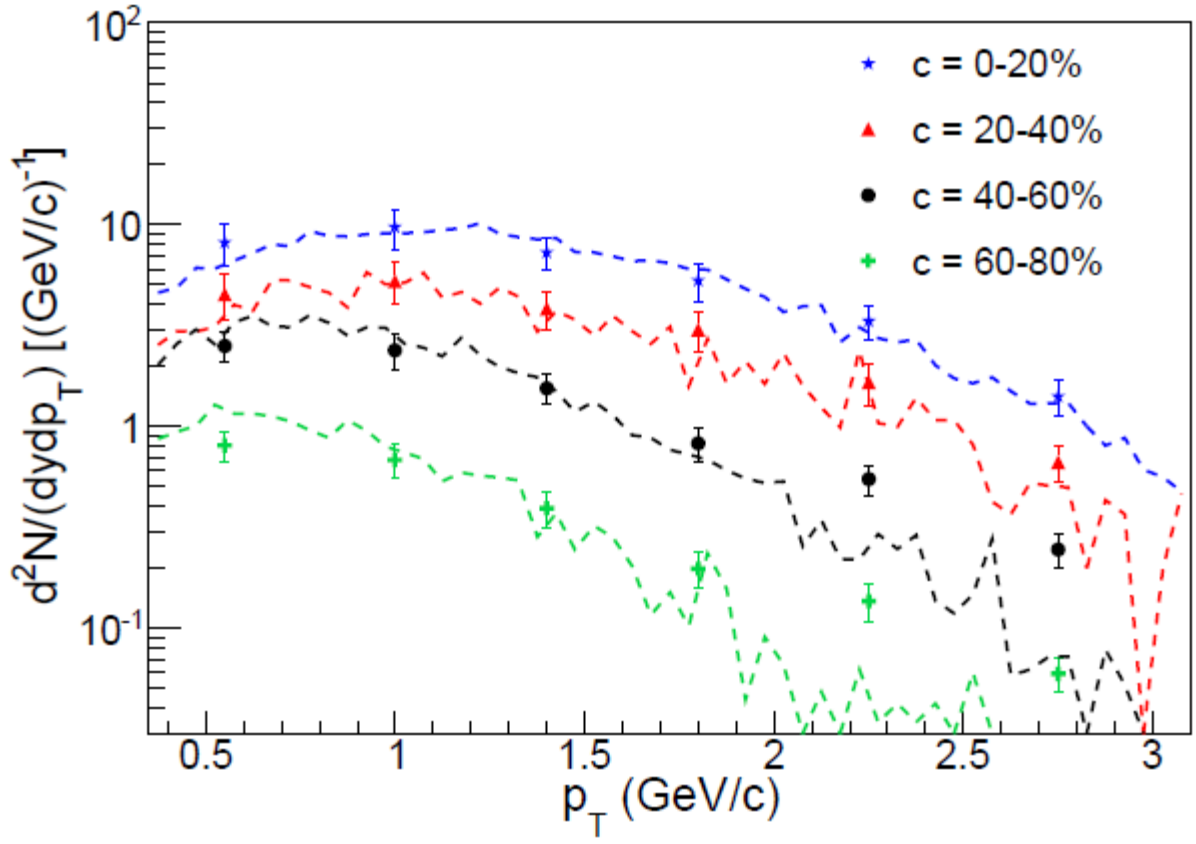

The $K(892)^*$ resonance p_T spectra for Pb+Pb collision events with different centralities at the LHC energy $\sqrt{s_{NN}} = 2.76$ TeV obtained in iHKM simulations (lines) in comparison with the experimental data [6] (markers).

Spectra of ϕ (LHC)

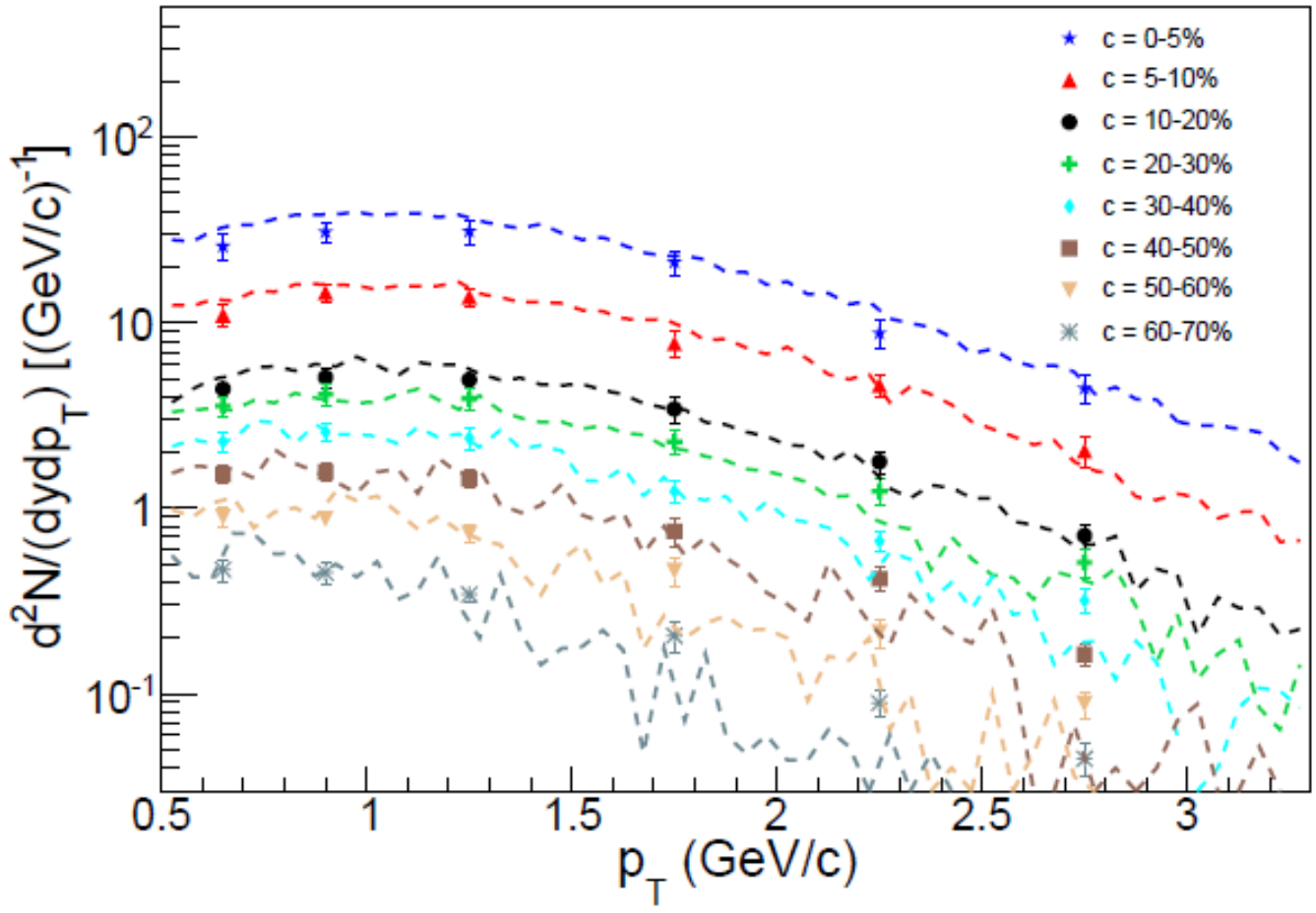

The $\phi(1020)$ resonance p_T spectra for Pb+Pb collision events with different centralities at the LHC energy $\sqrt{s_{NN}} = 2.76$ TeV obtained in iHKM simulations (lines) in comparison with the experimental data [6] (markers).

Some conclusions about particle productions

- Neither thermal nor chemical freeze-out cannot be considered as sudden at some corresponding temperatures.
- Particle yield probe ($\frac{dN_i}{d\eta}/\frac{dN_j}{d\eta}$ as well as absolute values $\frac{dN_i}{d\eta}$!) demonstrate that even at the minimal hadronization temperature $T_{ch} = T_h = 156$ MeV, the annihilation and other non-elastic scattering reactions play an important role in formation particle number ratios, especially, such where protons and pions are participating.
- It happens that the results for small and relatively large T_h are quite similar. It seems that inelastic processes (other than the resonance decays), that happen at the matter evolution below T_h , play a role of the compensatory mechanism in formation of $\frac{dN_i}{d\eta}/\frac{dN_j}{d\eta}$. Chemical f.-o. is continuous.
- As for the thermal freeze-out, the $K^{*0}(892)$ probes demonstrate that even 4-5 fm/c (proper time!) after hadronization 20-30% of decay products are still scattered.

Pair femtoscopic correlations: Bose-Einstein/Fermi-Dirac + final state interactions (BE/FD + FSI)

$$C(p,q) = 1 + \lambda \frac{\int d^4x_1 d^4x_2 g_1(x_1,p) g_2(x_2,p) \left(|\psi(\tilde{q},r)|^2 - 1 \right)}{\int d^4x_1 g_1(x_1,p_1) \int d^4x_2 g_2(x_2,p_2)} = 1 + \lambda \left\langle \left(|\psi(\tilde{q},r)|^2 - 1 \right) \right\rangle$$

where $\psi(\tilde{q},r)$ is reduced Bether-Salpeter amplitude, $r = x_1 - x_2, R = (x_1 + x_2)/2$

$$q = p_1 - p_2, p = (p_1 + p_2)/2 \qquad \tilde{q} = q - p(qp)/p^2$$

Pair femtoscopic correlations: Bose-Einstein/Fermi-Dirac + final state interactions (BE/FD + FSI)

$$C(p,q) = 1 + \lambda \frac{\int d^4x_1 d^4x_2 g_1(x_1,p) g_2(x_2,p) \left(|\psi(\tilde{q},r)|^2 - 1 \right)}{\int d^4x_1 g_1(x_1,p_1) \int d^4x_2 g_2(x_2,p_2)} = 1 + \lambda \left\langle \left(|\psi(\tilde{q},r)|^2 - 1 \right) \right\rangle$$

where $\psi(\tilde{q},r)$ is reduced Bether-Salpeter amplitude, $r = x_1 - x_2, R = (x_1 + x_2)/2$

$$q = p_1 - p_2, p = (p_1 + p_2)/2 \qquad \tilde{q} = q - p(qp)/p^2$$

For identical bosons (in smoothness approximation) with only Coulomb FSI

Y. Sinyukov, R. Lednicky, S.V. Akkelin, J. Pluta, B. Erazmus, Phys. Lett. B 432 (1998) 248.

$$C(p,q) = 1 - \lambda + \lambda \left\langle \left| \psi^c_{-\mathbf{k}*}(\mathbf{r}^*) \right|^2 \right\rangle (1 + \langle \cos(qx) \rangle) \rightarrow 1 + \lambda \langle \cos(qx) \rangle$$

where $\langle \cos(qx) \rangle = \exp(-q_{out}^2 R_{out}^2 - q_{side}^2 R_{side}^2 - q_{long}^2 R_{long}^2 - ...c.t.)$

$$\mathbf{k}^* = \mathbf{q}^*/2$$

$$\mathbf{r}* = \mathbf{x}_1^* - \mathbf{x}_2^*$$

Pair femtoscopic correlations: Bose-Einstein/Fermi-Dirac + final state interactions (BE/FD + FSI)

$$C(p,q) = 1 + \lambda \frac{\int d^4x_1 d^4x_2 g_1(x_1,p) g_2(x_2,p) \left(|\psi(\tilde{q},r)|^2 - 1\right)}{\int d^4x_1 g_1(x_1,p_1) \int d^4x_2 g_2(x_2,p_2)} = 1 + \lambda \left\langle \left(|\psi(\tilde{q},r)|^2 - 1\right) \right\rangle$$

where $\psi(\tilde{q},r)$ is reduced Bether-Salpeter amplitude, $r = x_1 - x_2, R = (x_1 + x_2)/2$

$$q = p_1 - p_2, p = (p_1 + p_2)/2 \qquad \tilde{q} = q - p(qp)/p^2$$

For identical bosons (in smoothness approximation) with only Coulomb FSI

Y. Sinyukov, R. Lednicky, S.V. Akkelin, J. Pluta, B. Erazmus, Phys. Lett. B 432 (1998) 248.

$$C(p,q) = 1 - \lambda + \lambda \left\langle \left|\psi^c_{-\mathbf{k}*}(\mathbf{r}^*)\right|^2 \right\rangle (1 + \langle \cos(qx) \rangle) \rightarrow 1 + \lambda \langle \cos(qx) \rangle$$

where $\langle \cos(qx) \rangle) = \exp(-q^2_{out}R^2_{out} - q^2_{side}R^2_{side} - q^2_{long}R^2_{long} - ...c.t.)$ $\quad \mathbf{k}^* = \mathbf{q}^*/2$ $\quad \mathbf{r}* = \mathbf{x}^*_\mathbf{1} - \mathbf{x}^*_\mathbf{2}$

Correlation functions in semi-classical events generators BE correlation:

$$C(\vec{q}) = \frac{\sum_{i \neq j} \delta_\Delta(\vec{q} - p_i + p_j)(1 + cos(p_j - p_i)(x_j - x_i))}{\sum_{i \neq j} \delta_\Delta(\vec{q} - p_i + p_j)}$$

where $\delta_\Delta(x) = 1$ if $|x| < \Delta p/2$ and 0 otherwise, with Δp being the bin size in histograms.

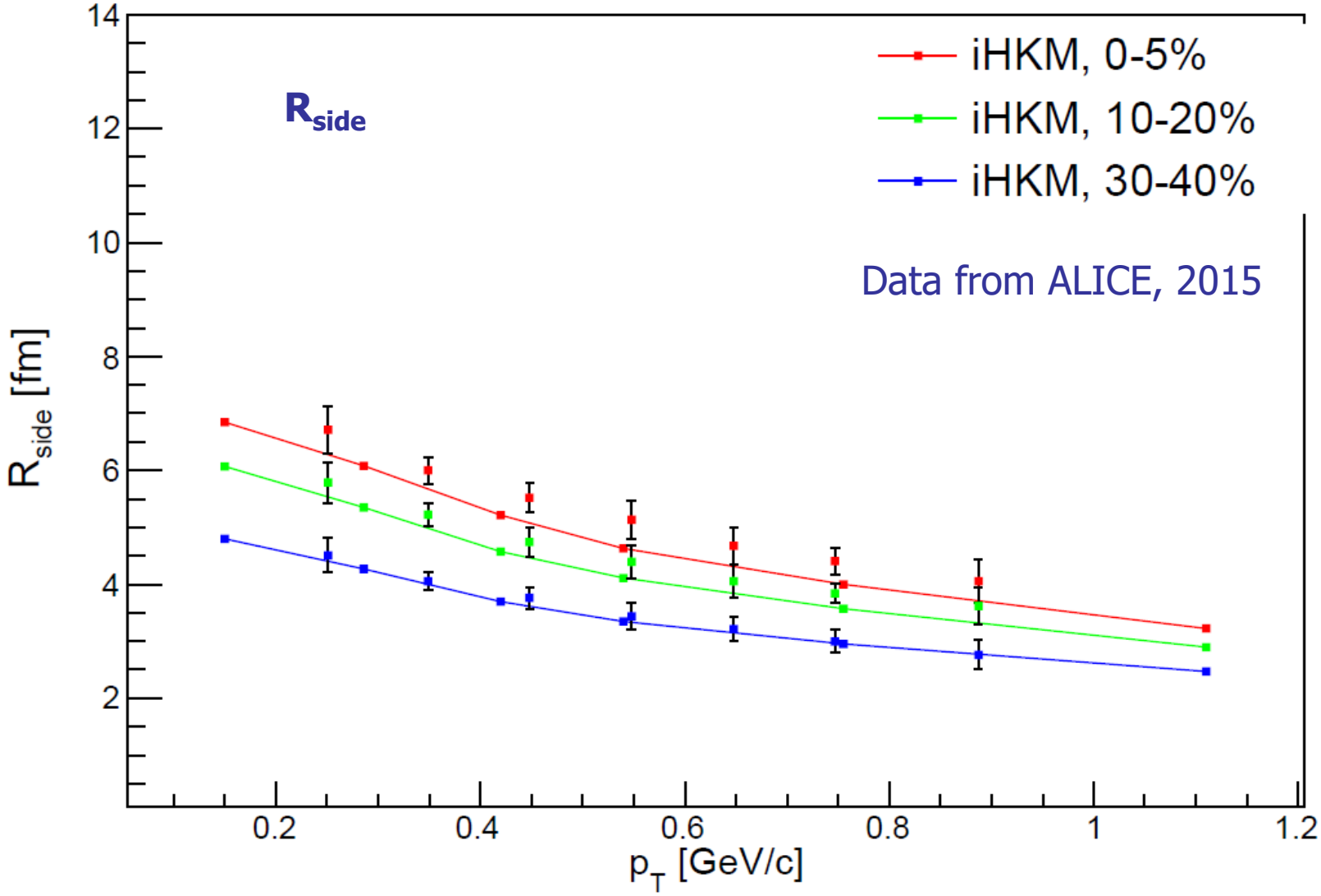

The R_{side} dependence on transverse momentum for different centralities in the iHKM scenario under the same conditions as in Fig. 1. The experimental data are from [33].

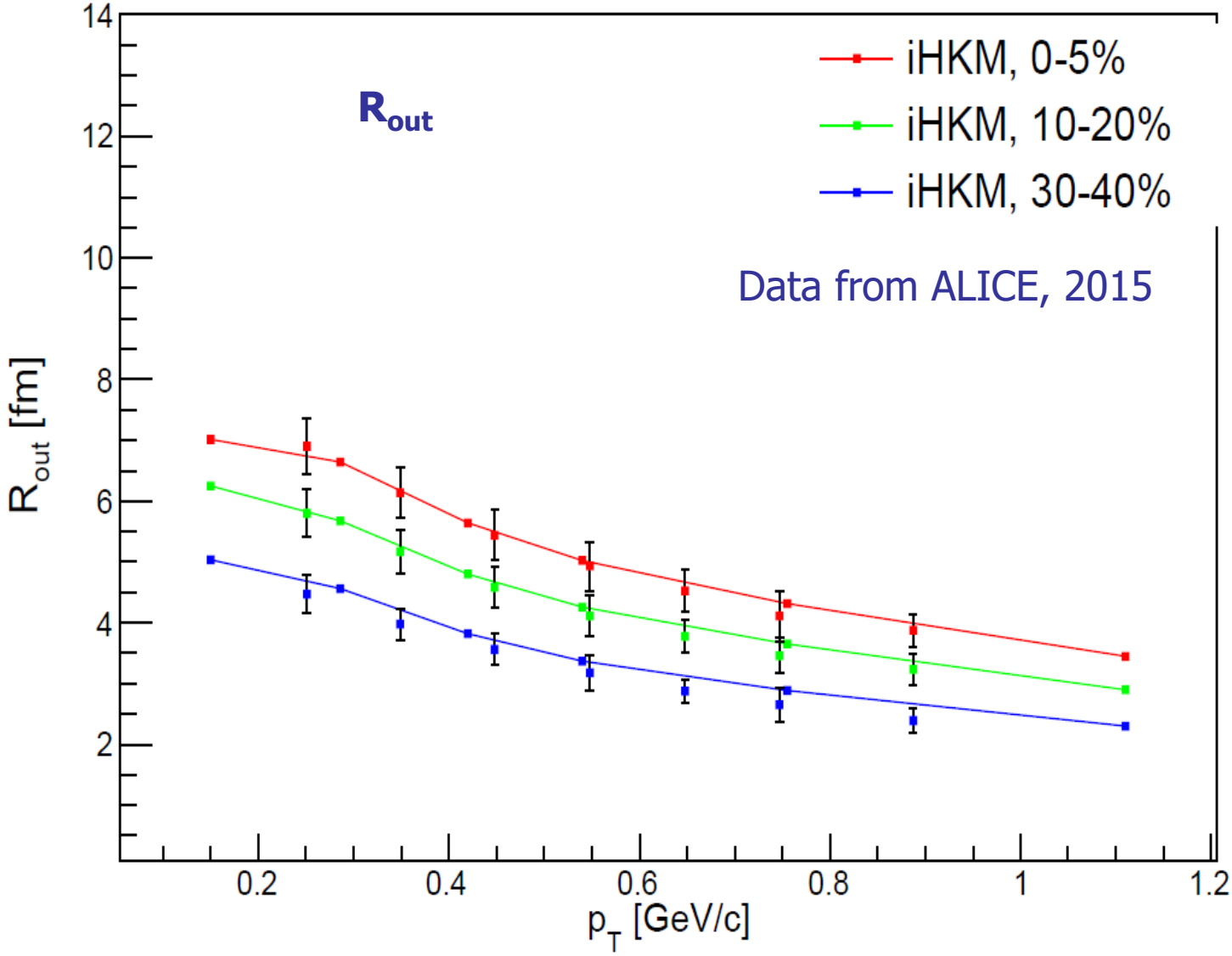

The R_{out} dependence on transverse momentum for different centralities in the iHKM basic scenario under the same conditions as in Fig. 1.

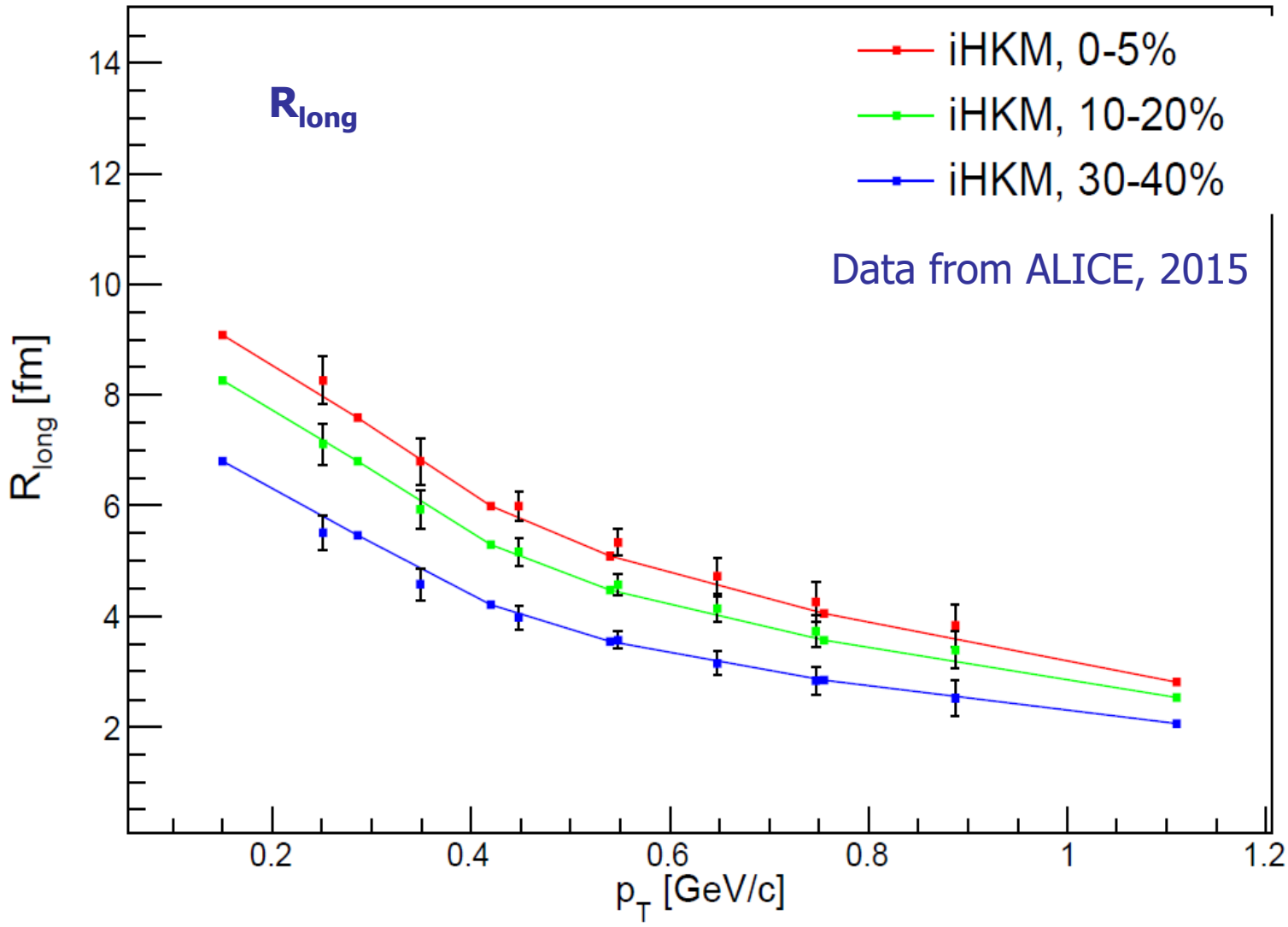

The R_{long} dependence on transverse momentum for different centralities in the iHKM basic scenario - the same conditions as in Fig. 1. The experimental data are from [33].

HKM predictions for kaon femtoscopy

Freeze-out Dynamics via Charged Kaon Femtoscopy in $\sqrt{s_{NN}}$=200 GeV Central Au+Au Collisions

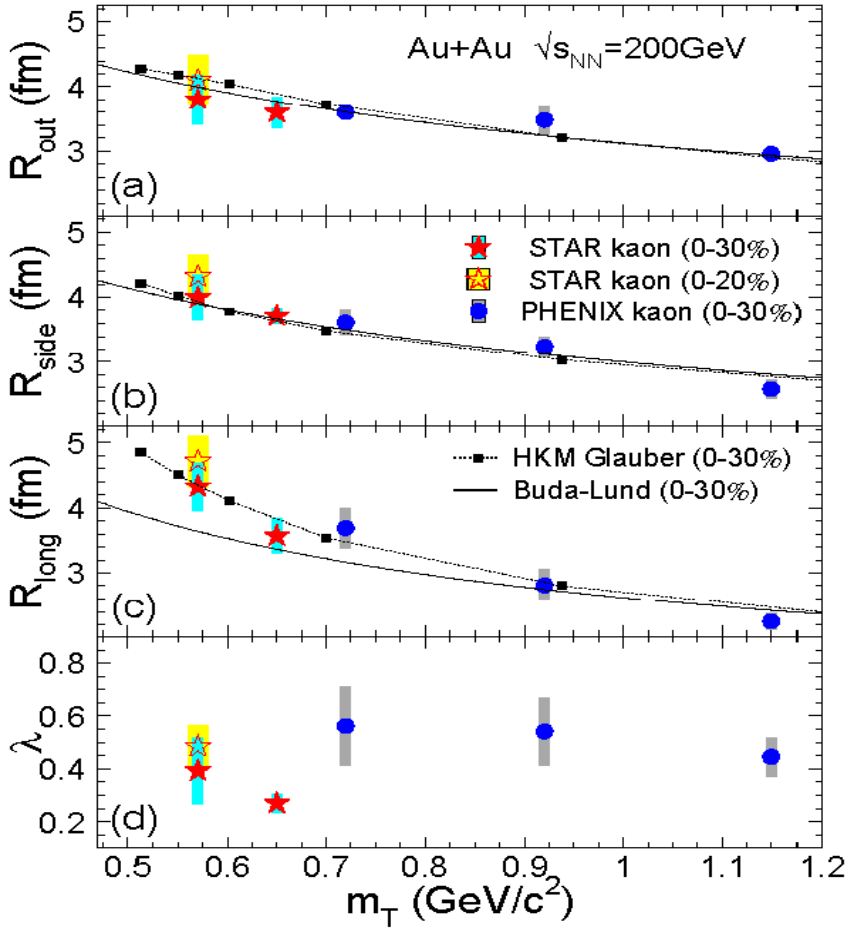

FIG. 4. Transverse mass dependence of Gaussian radii (a) R_{out}, (b) R_{side} and (c) R_{long} for mid-rapidity kaon pairs from the 30% most central Au+Au collisions at $\sqrt{s_{NN}}$=200 GeV. STAR data are shown as solid stars; PHENIX data [10] as solid circles (error bars include both statistical and systematic uncertainties). Hydro-kinetic model [23] with initial Glauber condition and Buda-Lund model [22] calculations are shown by solid squares and solid curves, respectively.

STAR Collaboration

arXiv:1302.3168 February 2013

Quotations:

Our measurement at $0.2 \leq k_T \leq 0.36$ GeV/c clearly favours the HKM model as more representative of the expansion dynamics of the fireball.

.....

In the outward and sideward directions, this decrease is adequately described by m_T–scaling. However, in the longitudinal direction, the scaling is broken. The results are in favor of the hydro-kinetic predictions [23] over pure hydrodynamical model calculations.

.....

[23] I. A. Karpenko and Y. M. Sinyukov, Phys. Rev. C **81** (2010) 054903.

$K^{\pm}K^{\pm}$ and $K^0_sK^0_s$ in Pb-Pb: HKM model

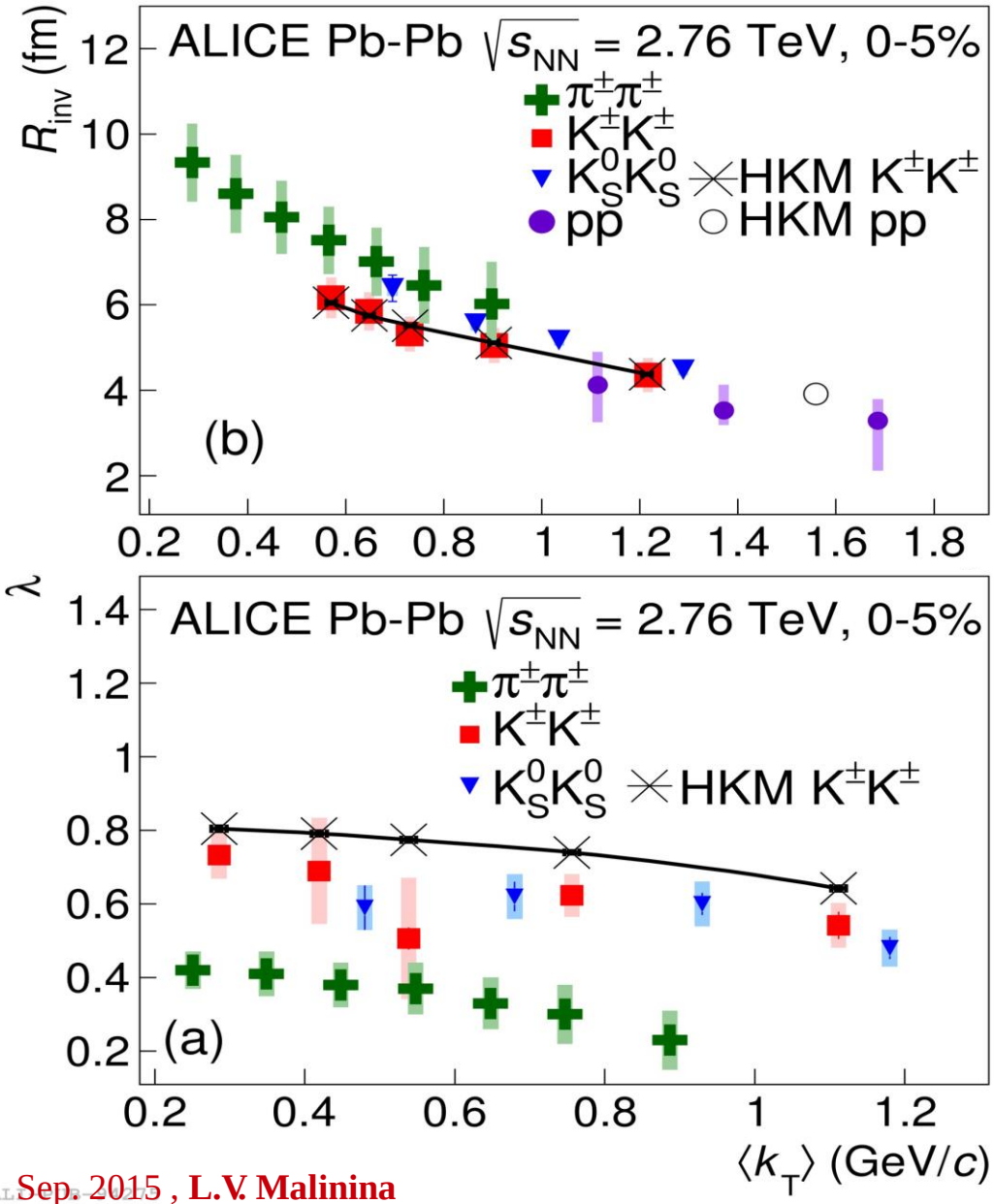

New results from ArXiv.org:1506.07884

- R and λ for $\pi^{\pm}\pi^{\pm}$, $K^{\pm}K^{\pm}$, $K^0_sK^0_s$, pp for 0-5% centrality
- Radii for kaons show good agreement with HKM predictions for $K^{\pm}K^{\pm}$
  (V. Shapoval, P. Braun-Munzinger, Yu. Sinyukov Nucl.Phys.A929 (2014))

- λ decrease with k_T, both data and HKM
- HKM prediction for λ slightly overpredicts the data
- Λ_π are lower λ_K due to the stronger influence of resonances

Comparison with HKM for 0-5% centrality

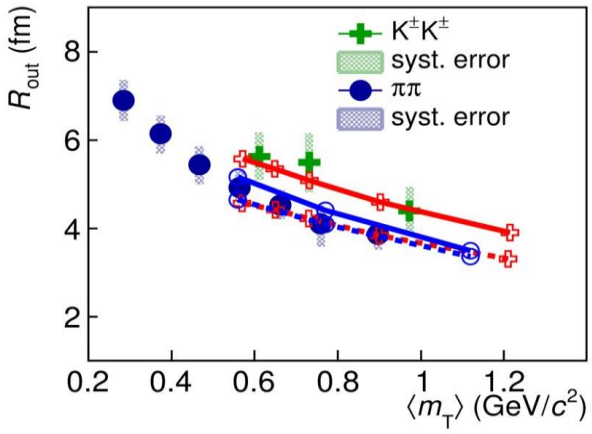

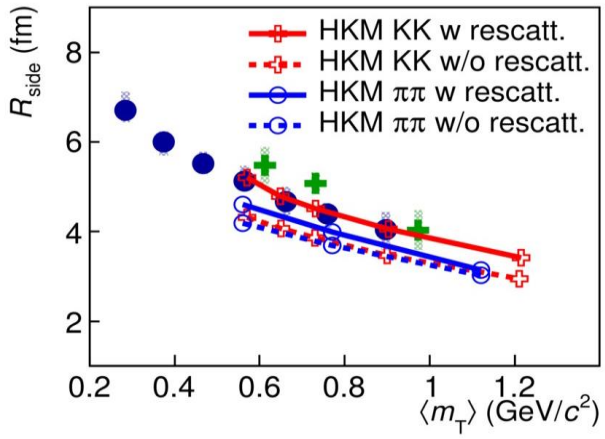

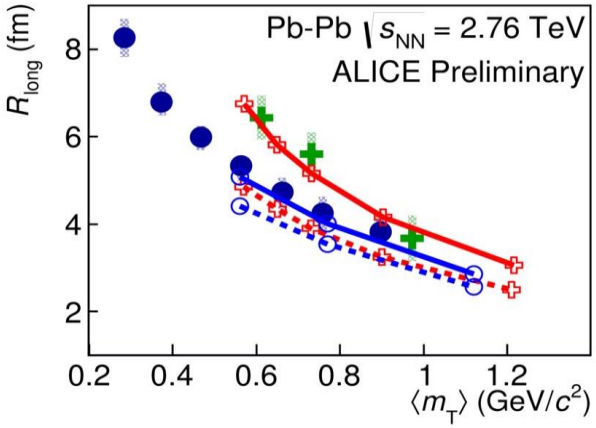

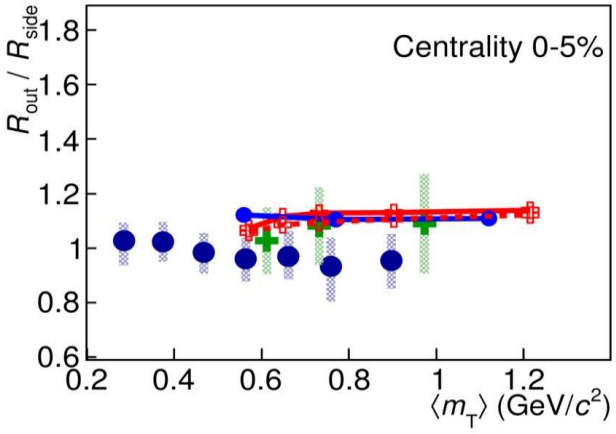

ALI-PREL-96575

- HKM model slightly underestimates R_{side} $\rightarrow$ overestimates R_{out}/R_{side} ratio for π

- HKM model with re- scatterings (M. Shapoval, P. Braun-Munzinger, Iu.A. Karpenko, Yu.M. Sinyukov, Nucl.Phys. A 929 (2014) 1.) describes well ALICE π & K data.

- HKM model w/o re-scatterings demonstrates approximate m_T scaling for π & K, but does not describe ALICE π & K data

- The observed deviation from m_T scaling is explained in (M. Shapoval, P. Braun-Munzinger, Iu.A. Karpenko, Yu.M. Sinyukov, Nucl.Phys. A 929 (2014) by essential transverse flow & re-scattering phase.

3D $K^{\pm}K^{\pm}$ & $\pi\pi$ radii versus k_T

Pion results from ArXiv.org:1507.06842

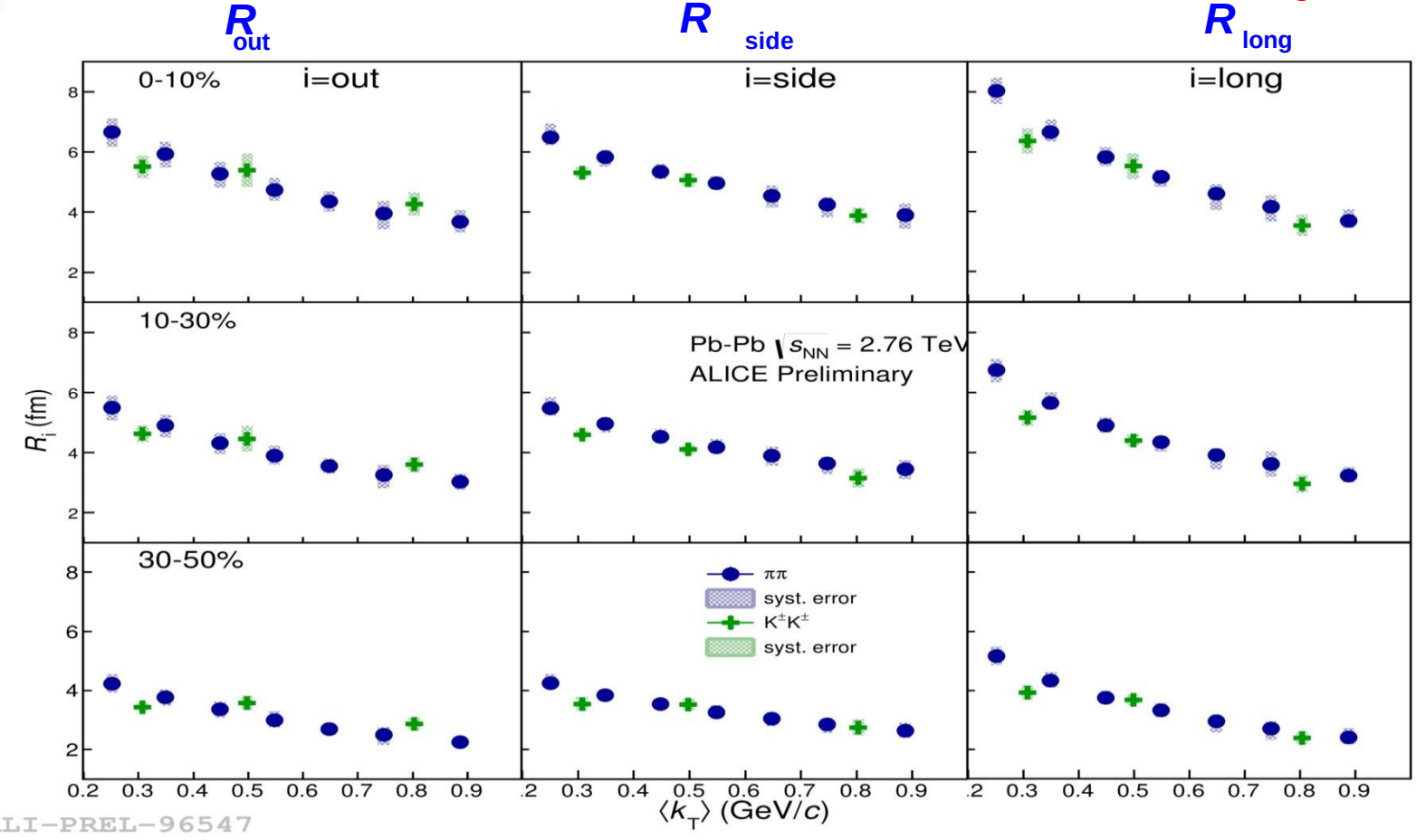

- Radii scale better with k_T than with m_T according with HKM predictions

  (V. Shapoval, P. Braun-Munzinger, Iu.A. Karpenko, Yu.M. Sinyukov, Nucl.Phys. A 929 (2014) 1);

- Similar observations were reported by PHENIX at RHIC (arxiv:1504.05168).

Space-time picture of the pion and kaon emission

$$\underbrace{R_l^2(k_T) = \tau^2\lambda^2\left(1+\frac{3}{2}\lambda^2\right)}_{\text{2015}} \approx \text{w/o transv. expansion} \approx \underbrace{\tau^2\frac{T}{m_T}}_{\text{1987}}\underbrace{\frac{K_2(\frac{m_T}{T})}{K_1(\frac{m_T}{T})}}_{\text{1995}}$$

where $\lambda^2 = \frac{T}{m_T}\left(1-\frac{\overbrace{k_T^2}^{\bar{v}_T^2}}{(m_T+\alpha T)^2}\right)^{1/2}$

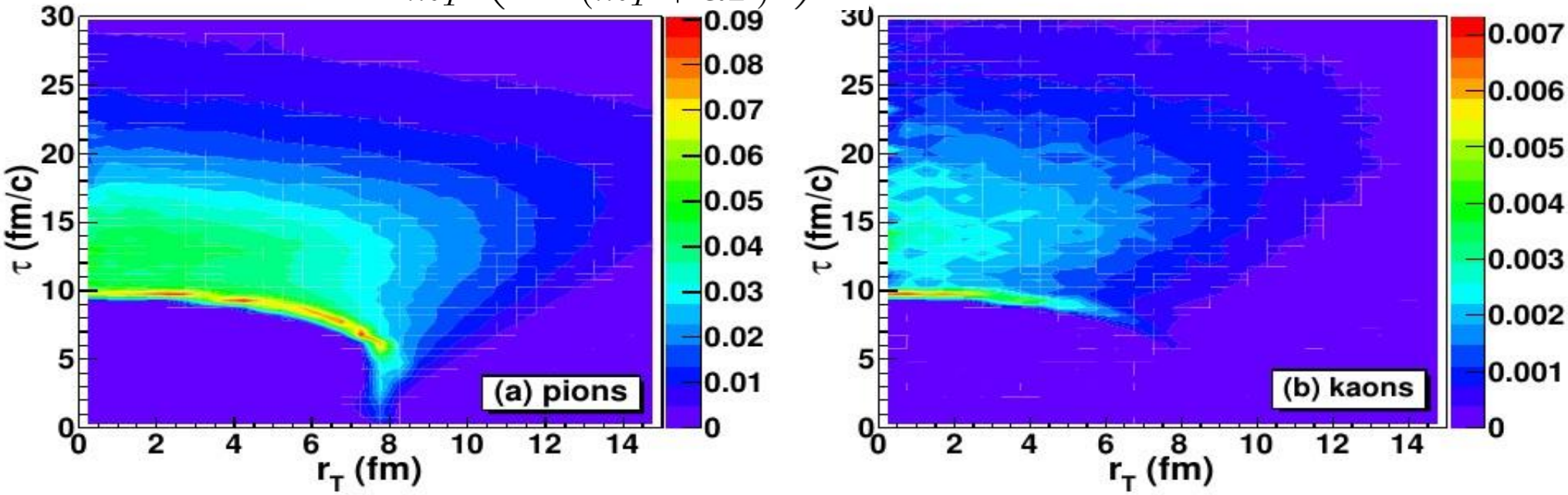

FIG. 4. The momentum angle averaged emission functions per units of space-time and momentum rapidities $g(\tau, r_T, p_T)$ [fm^{-3}] (see body text) for pions (a) and kaons (b) obtained from the HKM simulations of Pb+Pb collisions at the LHC $\sqrt{s_{NN}} = 2.76$ GeV, $0.2 < p_T < 0.3$ GeV/c, $|y| < 0.5$, $c = 0-5\%$.

From Yu.S., Shapoval, Naboka, Nucl. Phys. A 946 (2016) 247 (arXiv:1508.01812)

Extraction of emission time from fit R_{long} T

- The new formula for extraction of the maximal emission time for the case of strong transverse flow was used (Yu. S., Shapoval, Naboka, Nucl. Phys. A 946 (2016) 227)

- The parameters of freeze-out: T and "intensity of transverse flow" α were fixed by fitting π and K spectra (arxiv:1508.01812)

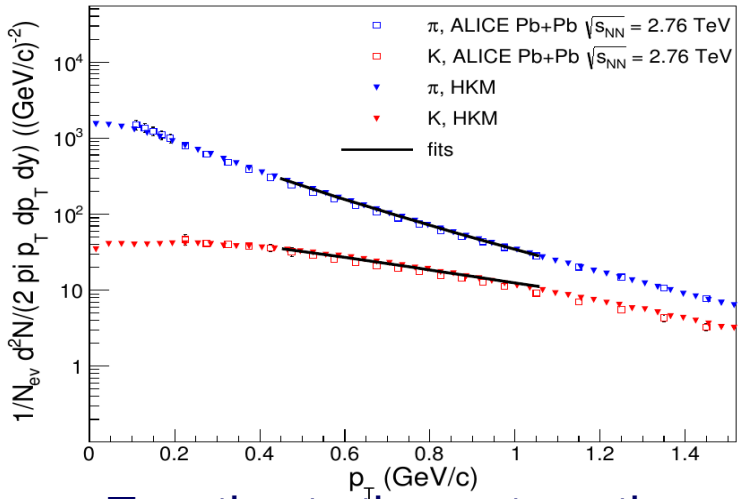

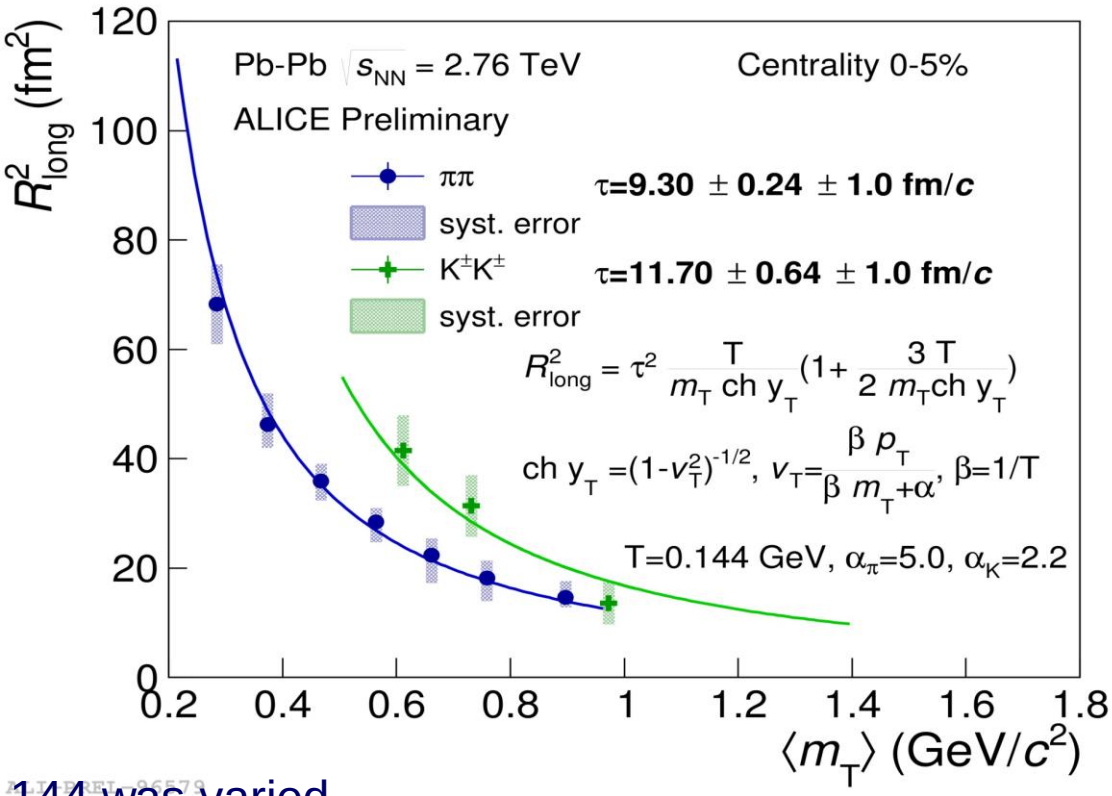

- To estimate the systematic errors: T = 0.144 was varied on ± 0.03 GeV & free α_π, α_K, were used; systematic errors ~ 1 fm/c

- Indication: $\tau_\pi < \tau_K$. Possible explanations (arxiv:1508.01812): HKM includes re-scatterings (UrQMD cascade): e.g. Kπ→K*(892)→Kπ, KN→K*(892)X; (K*(892) lifetime 4-5 fm/c) [πN→N*(Δ)X, N*(Δ)→πX (N*s(Δs)- short lifetime)]

Source function S(r*)

Integrated in time distribution of the pairs on relative distance between particles in the pairs in the rest frames of the pairs

The correlation function in smoothness approximation

$$C(p,q) = 1 + \frac{\int d^4x_1 d^4x_2 g_1(x_1,p_1) g_2(x_2,p_2) \left(|\psi(\tilde{q},r)|^2 - 1 \right)}{\int d^4x_1 g_1(x_1,p_1) \int d^4x_2 g_2(x_2,p_2)}$$

where $\psi(\tilde{q},r)$ is reduced Bether-Salpeter amplitude, $r = x_1 - x_2, R = (x_1 + x_2)/2$

$$q = p_1 - p_2, p = (p_1 + p_2)/2 \qquad \tilde{q} = q - p(qp)/p^2$$

The relative distance distribution function

$$s(r,p_1,p_2) = \frac{\int d^4R g_1(R + r/2, p_1) g_2(R - r/2, p_2)}{\int d^4R g_1(R,p_1) \int d^4R g_2(R,p_2)} = \int d^4R \tilde{g_1}(R + r/2, \frac{2m_1}{m_1+m_2}p) \tilde{g_2}(R - r/2, \frac{2m_2}{m_1+m_2}p) = s(r,p)$$

Main contribution to $C(p_1,p_2)$ is at $\mathbf{v}_1 \approx \mathbf{v}_2$

$$\underbrace{C(\mathbf{q}^*, \mathbf{p}{=}\mathbf{0}) - 1}_{R(\mathbf{q})} = \int d^3r^* \int \underbrace{dt^* s(r^*, \mathbf{0})}_{S(\mathbf{r}^*)} (|\psi(\mathbf{r}^*, \mathbf{q}^*)|^2 - 1) = \int d^3r^* \underbrace{S(\mathbf{r}^*)}_{e^{-r^2/4r_0^2}} \overbrace{K(\mathbf{r}^*, \mathbf{q}^*)}^{f_0 \ d_0 \ a}$$

m_T scaling of source radii for meson and baryon pairs because in pair rest frame the transverse flow are absent

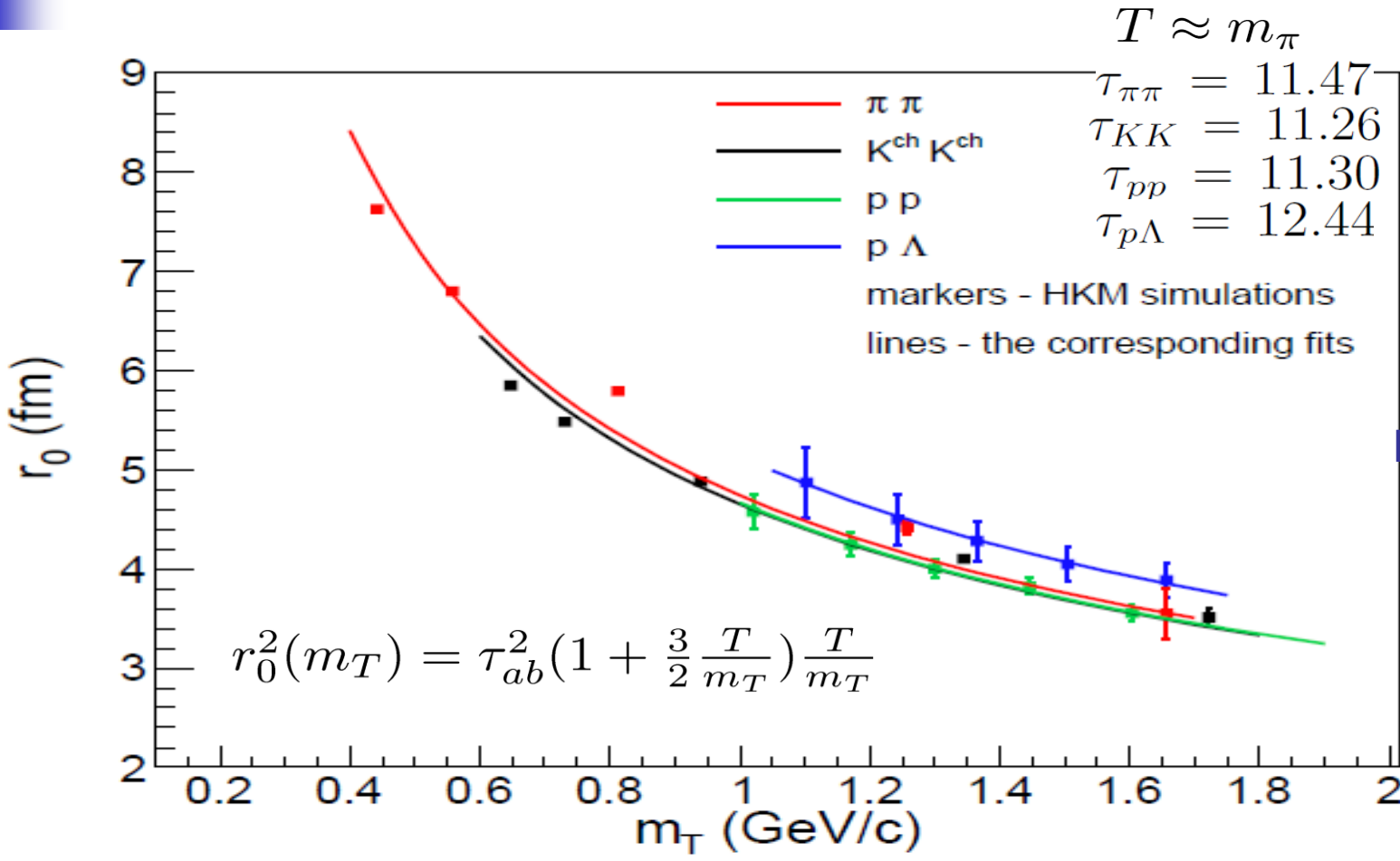

Yu.S., Shapoval, Naboka, Nucl. Phys. A 946 (2016) 247

The m_T dependencies of $\pi\pi$, $K^{ch}K^{ch}$, pp and $p\Lambda$ source radii r_0 extracted from corresponding angle-averaged source functions calculated in HKM for $\sqrt{s_{NN}} = 2.76$ GeV Pb+Pb collisions at the LHC, $c = 0 - 5\%$, $|\eta| < 0.8$. Transverse momentum ranges are $0.14 < p_T < 1.5$ GeV/c for pions and kaons, $0.7 < p_T < 4.0$ GeV/c for protons and $0.7 < p_T < 5.0$ GeV/c for Lambdas.

The $p-\Lambda \oplus \bar{p}-\bar{\Lambda}$ correlation function (RHIC)

F. Wang, S. Pratt, Phys. Rev. Lett. 83, 3138 (1999)

$f_0^s = 2.88$ fm, $f_0^t = 1.66$ fm, $d_0^s = 2.92$ fm, $d_0^t = 3.78$ fm

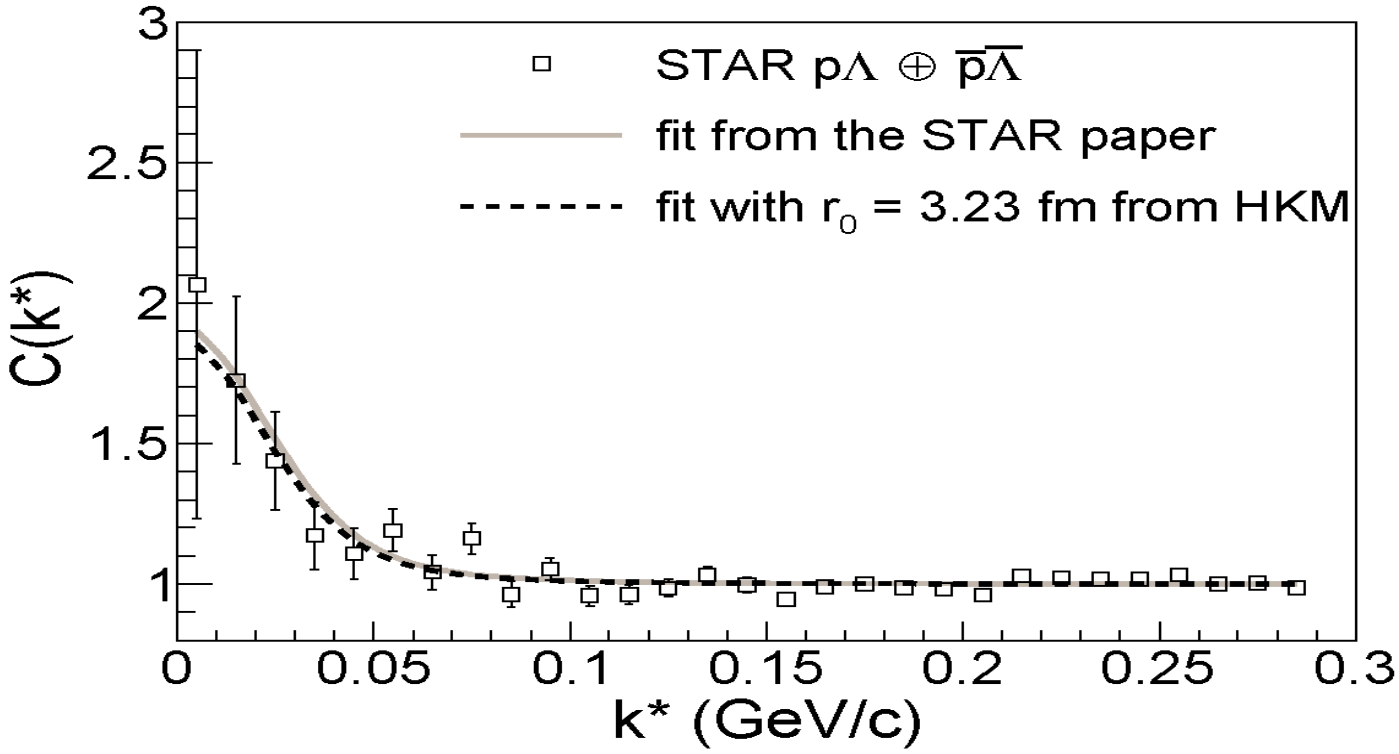

Scattering lengths f_0

"Effective radius" d_0

Shapoval, Erazmus, Lednicky, and Yu.S. Phys. Rev. C **92**, 034910 (2015)

The $p-\Lambda \oplus \bar{p}-\bar{\Lambda}$ correlation function measured by STAR (open markers), the corresponding fit according to (6) with parameters fixed as in the STAR paper [4] within the Lednický and Lyuboshitz analytical model [1] (light solid line) and our fit within the same model with the source radius r_0 extracted from the HKM calculations (dark dashed line).

The $\bar{p}-\Lambda \oplus p-\bar{\Lambda}$ correlation function RHIC

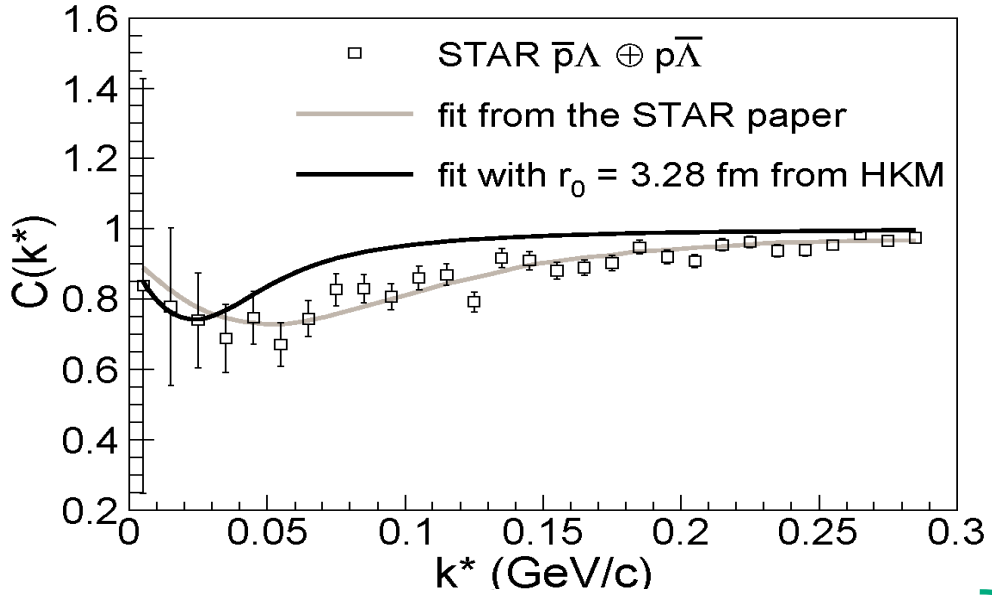

$$\text{STAR: } \Re f = -2.03 \pm 0.96^{+1.37}_{-0.12} \text{ fm},$$
$$\Im f = 1.01 \pm 0.92^{+2.43}_{-1.11} \text{ fm},$$
$$r_0 = 1.50 \pm 0.05^{+0.10}_{-0.12} \pm 0.3 \text{ fm}$$

$$C_{meas}(k^*) = \lambda(k^*)C(k^*) + (1-\lambda(k^*))$$

Residual correlations

$$C_{uncorr}(k^*) = 1 + \lambda(k^*)(C(k^*)-1) + \alpha(k^*)(C_{res}(k^*)-1)$$

$$C_{res}(k^*) = 1 - \tilde{\beta}e^{-4k^{*2}R^2} \quad \tilde{\alpha}(1-\lambda(k^*))$$

$$\Re f_0 = 0.14 \pm 0.66 \text{ fm},$$

$$\Im f_0 = 1.53 \pm 1.31 \text{ fm}, \ \beta = \tilde{\alpha}\tilde{\beta} = 0.034 \pm 0.005$$

and $R = 0.48 \pm 0.05$ fm, with $\chi^2/\text{ndf} = 0.87$.

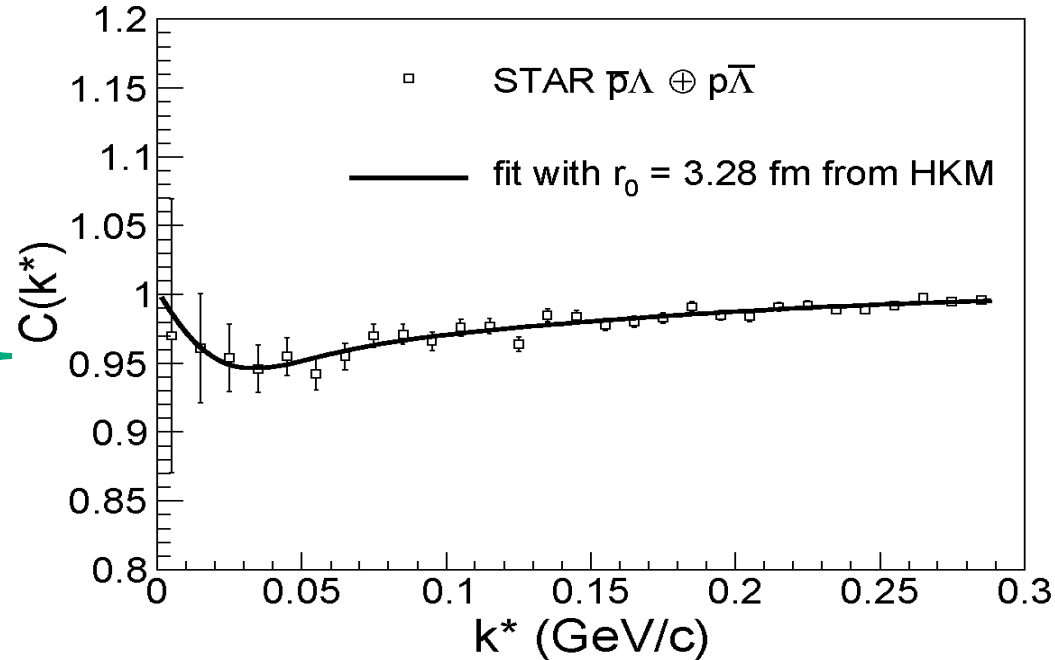

The $p-\Lambda \oplus \bar{p}-\bar{\Lambda}$ correlation function (prediction for LHC)

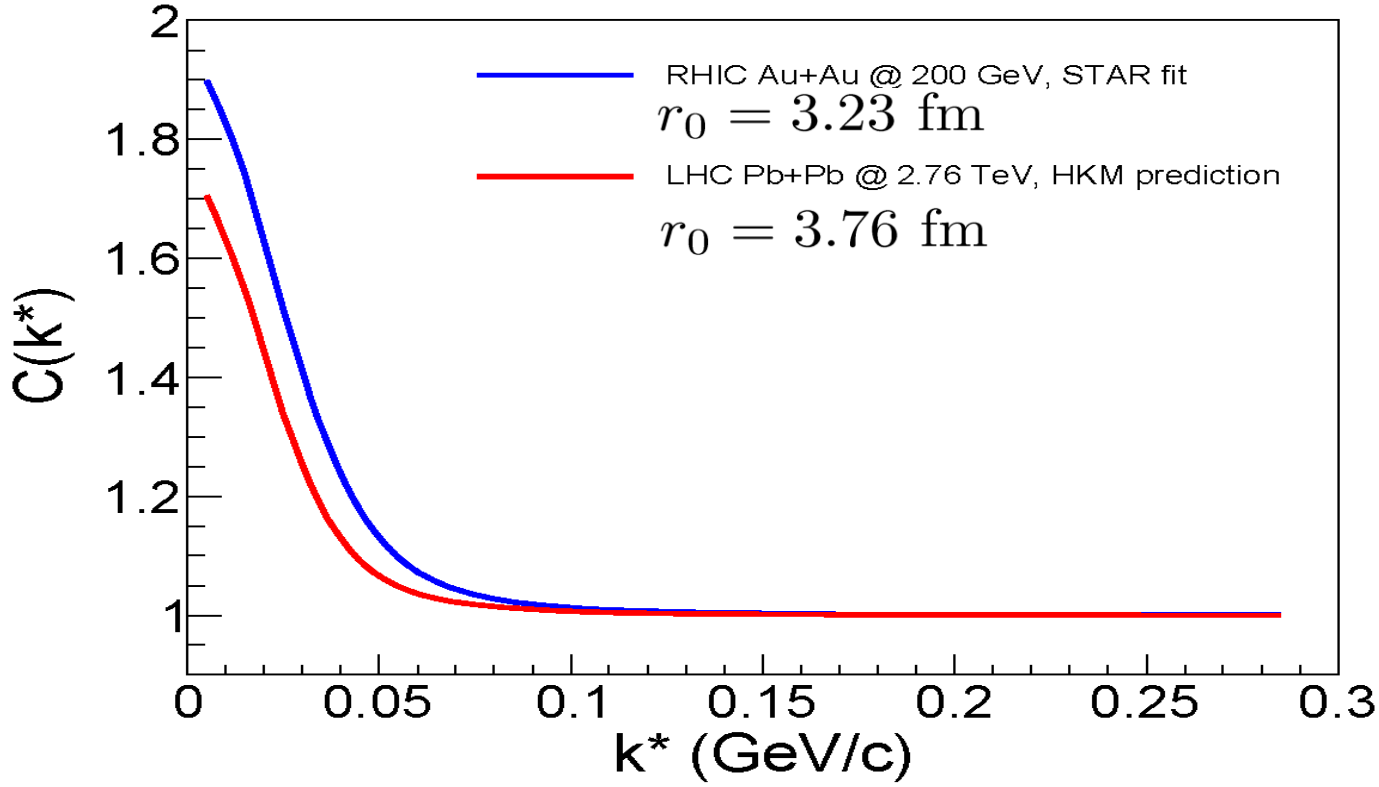

Shapoval, Yu. S. , Naboka

Phys. Rev. C **92**, 044910 (2015)

Scattering lengths f_0

"Effective radius" d_0

are the same as at RHIC

The HKM prediction for purity corrected $p-\Lambda \oplus \bar{p}-\bar{\Lambda}$ correlation function in the LHC Pb+Pb collisions at $\sqrt{s_{NN}} = 2.76$ TeV, $c = 0-5\%$, $|\eta| < 0.8$, with $0.7 < p_T < 4$ GeV/c for protons and $0.7 < p_T < 5$ GeV/c for lambdas (red line). The LHC source radius value calculated in HKM is $r_0 = 3.76$ fm. The Lednický-Lyuboshitz fit to the top RHIC energy correlation function, corresponding to the STAR experiment [8], with $r_0 = 3.23$ fm extracted from the HKM source function is presented for comparison (blue line).

The $\bar{p}-\Lambda \oplus p-\bar{\Lambda}$ correlation function (prediction for LHC)

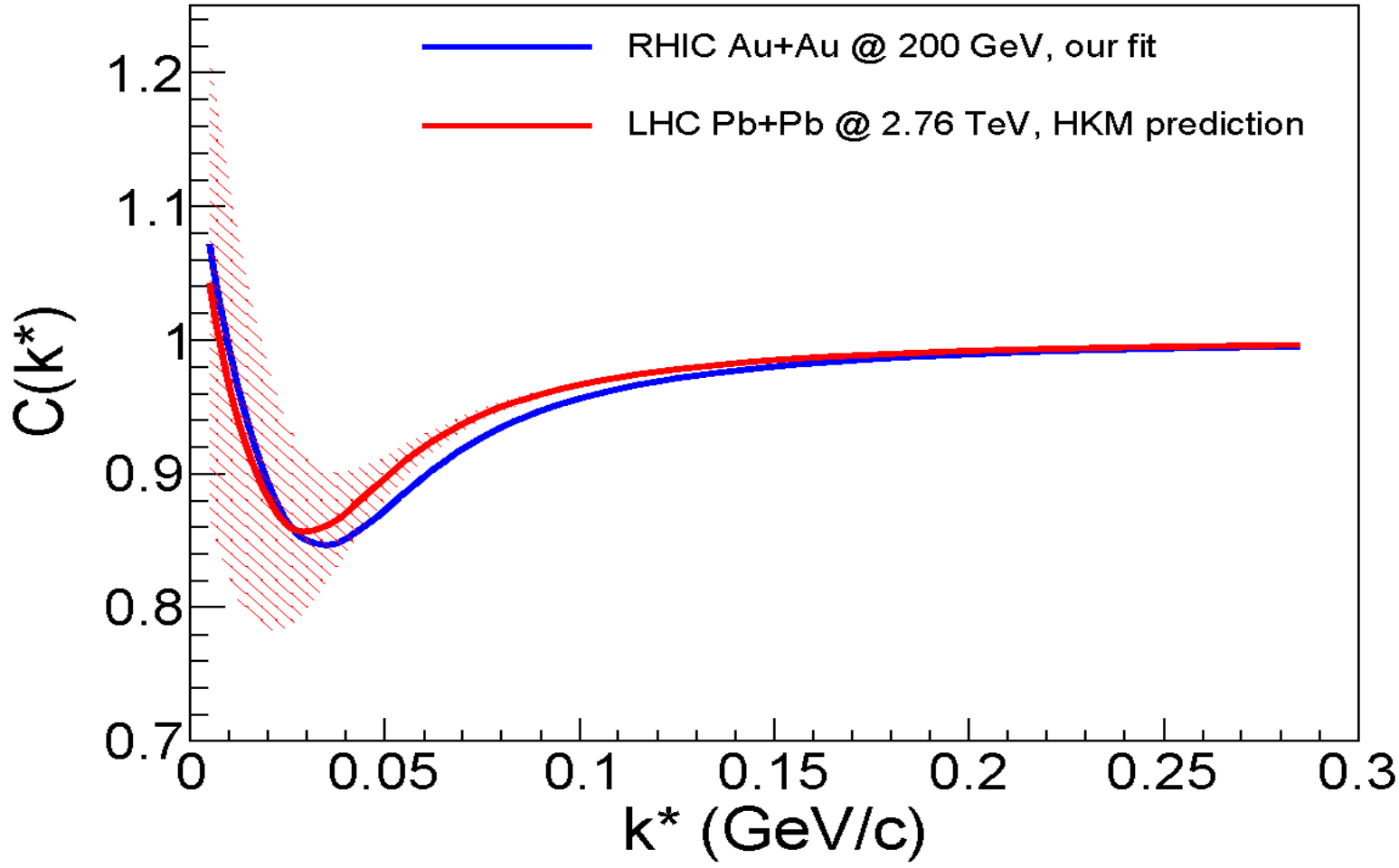

The same as in previous two figures, but the correlation functions are corrected for purity and residual correlations, i. e. $C(k^*) = 1 + (C_{uncorr}(k^*) - 1)/\lambda(k^*) - \alpha(k^*)(C_{res}(k^*) - 1)/\lambda(k^*)$.

"Pure" correlation function for $p - \Xi^- \oplus \bar{p} - \Xi^+$ (prediction for the LHC)

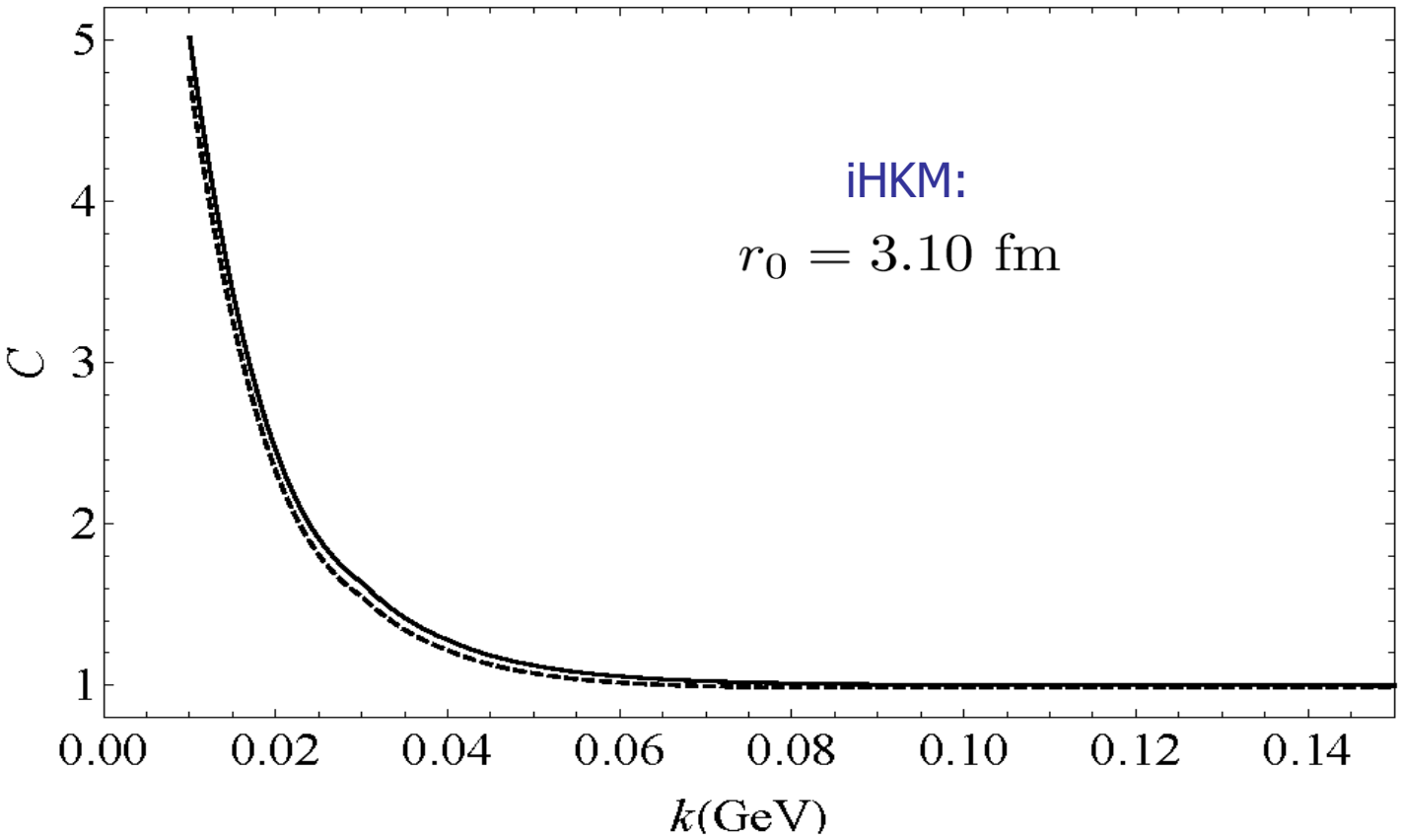

Scattering lengths f_0

"Effective radius" d_0

are supposed to be as for baryon-baryon pairs

$p - \Lambda \oplus \bar{p} - \bar{\Lambda}$

The pure (purity $\lambda = 1$) baryon-baryon correlation function between primary proton and cascade, $p\Xi^-$ obtained in iHKM simulations. The Gaussian radius in the source function distribution in iHKM is 3.1 fm. The scattering lengths for strong interactions are supposed to be the same as in $p - \Lambda$ systems. The solid line is related to utilizing the basic formula (1) for the Coulomb plus strong FSI at all distances r between the two baryons in the rest system of the pair. The dashed line corresponds to switching off all interactions at $r < 1fm$. Therefore, the realistic results, accounting for the baryon kernel in short range interaction and electromagnetic form-factors of barvons is supposed to be between these two curves.

Measured $p - \Xi^- \oplus \bar{p} - \Xi^+$ correlation function (prediction for LHC)

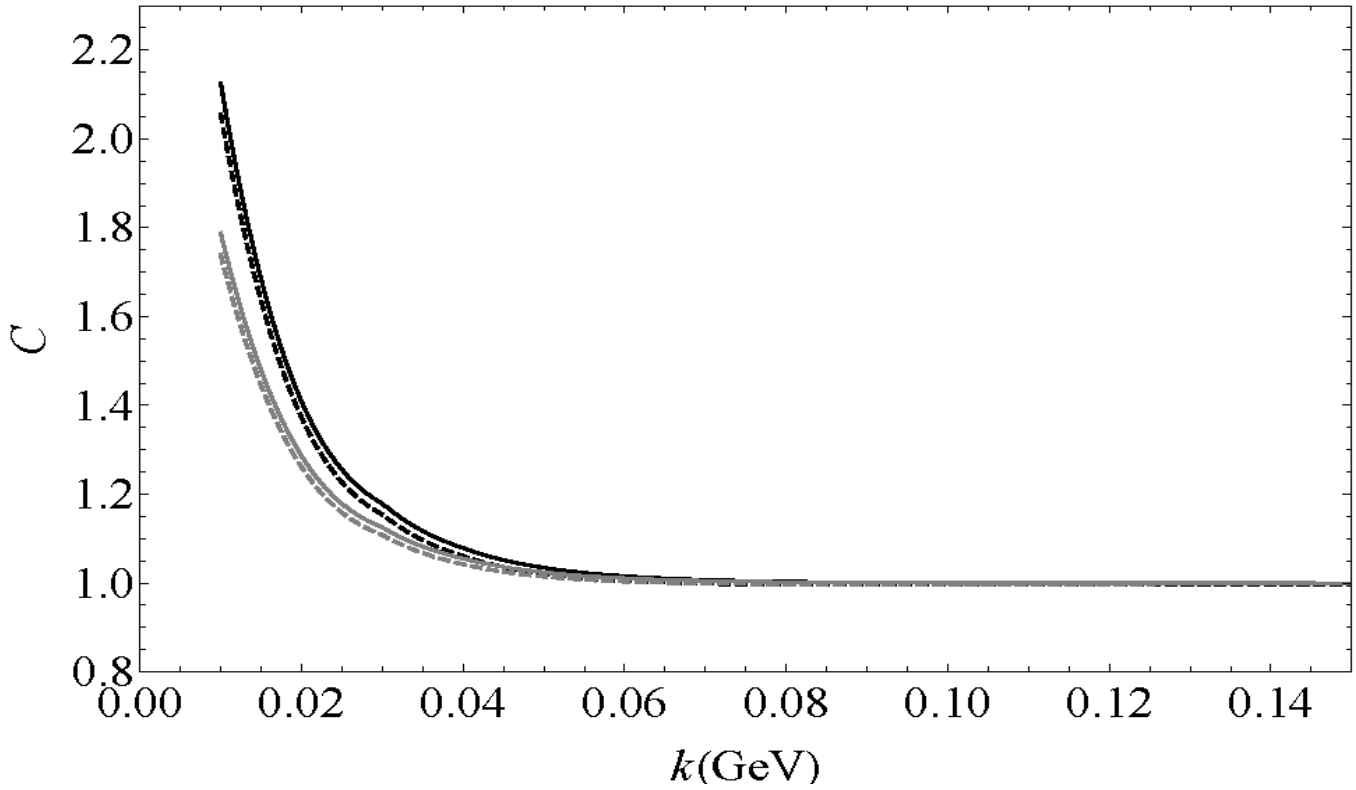

The prediction for observed baryon-baryon correlation function proton and cascade, $p\Xi^-$ obtained in iHKM simulations. The purity that is result of long-lived resonance decays is found in iHKM as $\lambda_{res} = 0.28$. The gray lines account for purity connected with particle misidentification and some other detector aspects. We put this additional factor as 0.7, so that the gray lines are corresponding to $\lambda = 0.7\lambda_{res} = 0.196$.

Baryon – antibaryon correlations $\bar{p} - \Xi^- \oplus p - \Xi^+$ (prediction for the LHC)

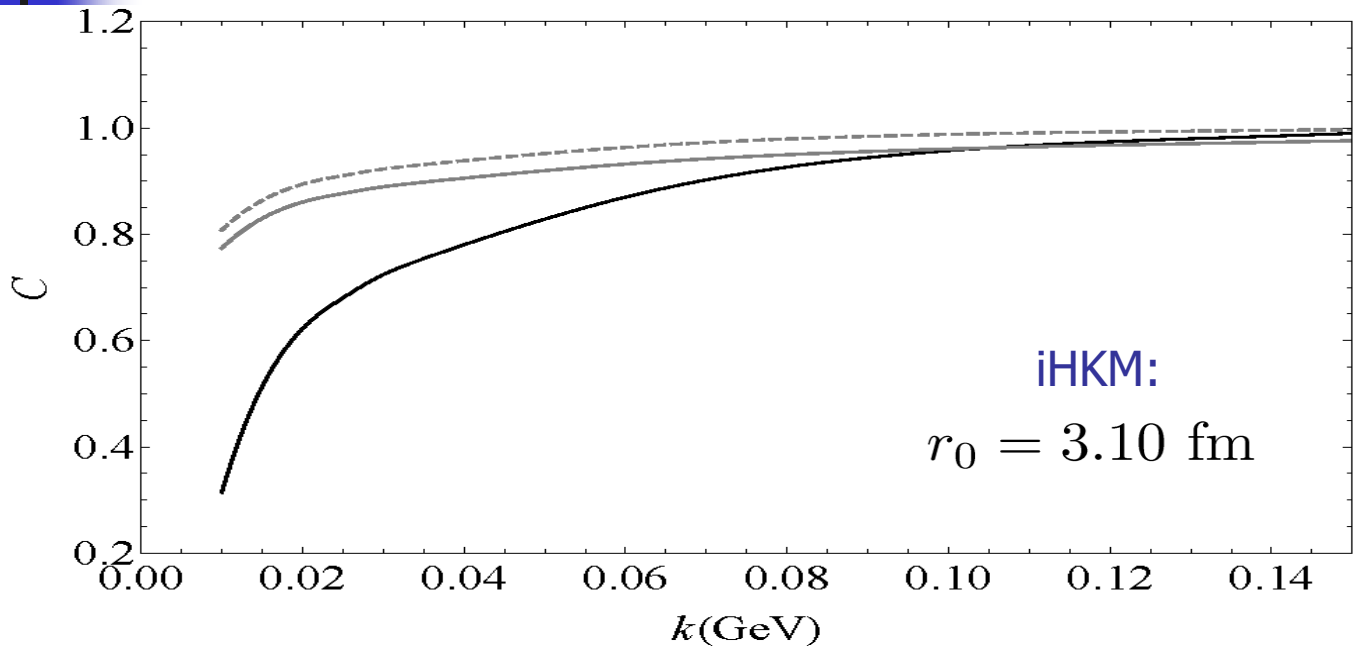

The baryon-antibaryon correlation function for primary proton and anti-cascade, $p\Xi^+$, obtained in iHKM simulations. The Gaussian radius in the source function distribution in iHKM is 3.1 fm. The scattering lengths for strong interactions are supposed to be the same as for $\overline{\Lambda}$ extracted from STAR data in Ref. [4]. The solid line is related to purity = 1 in primary baryon-antibaryon system. The gray dashed line correspond to the purity that is result of long-lived resonance decays as it found in iHKM, $\lambda_{res} = 0.28$. Solid gray line corresponds account for the residual correlations among primary parents of p or/and Ξ^+. The parameters of such a correction are taken from top RHIC energies [4] and adjust for LHC space scale by using iHKM.

Summary (spectra and meson correlations)

- The integrated hydrokinetic model (iHKM) of A+A collisions is developed and tuned to satisfactory describe at different centralities the multiplicities, pion, kaon and antiproton spectra and elliptic flow of all charged particles.

- The results are not much sensitive to reasonable variations of shear viscosity, η/s relaxation time, τ_{rel}, time of thermalization τ_{th}, if their change is accompanied by re-scaling of the maximal initial energy density. But spectra are quite sensitive to the initial time τ_0 of (non-thermal) $T^{\mu\nu}(\tau_0)$ formation.

- The pion and kaon interferometry radii 1D and 3D are well described with above fixed parameters. The reasons for violation of m_T – scaling are intensive transverse flows and (mainly) re-scattering at the afterburner stage.
The HKM prediction for pion-kaon k_T -scaling is conformed at RHIC and LHC experiments.

- It is found that effective emission time of kaon radiation is larger then the corresponding for pions. It supposed to be conditioned by K* with life-time 4-5 fm/c. Its decays in hadronic medium results in suppression of the possibility of K* registration since the daughter particles are partially rescatter.
The results for K* (reduced 23% due to rescat.) and ϕ (increase 10% because of coalescence in UrQMD) as compare to their numbers at chemical freeze-out .

Summary (baryon correlations)

- Source functions extracted from iHKM, allows one to analyze the strong interaction in differen baryon– (anti)baryon systems, including also multi-strange ones using FSI technique.

- The analysis of $p-\Lambda \oplus \bar{p}-\bar{\Lambda}$ and $p-\Lambda \oplus \bar{p}-\bar{\Lambda}$ correlations at RHIC with the residual correlations taken into account and source function taken from iHKM, brings good description of the experimental results and allow to estimate the scattering lengths for $\bar{p}-\Lambda \oplus p-\bar{\Lambda}$

- The extracted at RHIC parameters, after the re-scaling for new energies, allow one to make prediction for the above hadron correlations at LHC within HKM.

- The first estimates for $\bar{p}-\Xi^{-} \oplus p-\Xi^{+}$ and $p-\Xi^{-} \oplus \bar{p}-\Xi^{+}$ within iHKM model are presented.

Acknowledgement

Щиро дякую усіх присутніх за їх присутність та увагу !

Thank you